



Measurement of the CP -violating phase ϕ_s in the $B_s^0 \rightarrow J/\psi \phi(1020) \rightarrow \mu^+ \mu^- K^+ K^-$ channel in proton-proton collisions at $\sqrt{s} = 13$ TeV

The CMS Collaboration*

Abstract

The CP -violating weak phase ϕ_s and the decay width difference $\Delta\Gamma_s$ between the light and heavy B_s^0 mass eigenstates are measured with the CMS detector at the LHC in a sample of 48 500 reconstructed $B_s^0 \rightarrow J/\psi \phi(1020) \rightarrow \mu^+ \mu^- K^+ K^-$ events. The measurement is based on a data sample corresponding to an integrated luminosity of 96.4 fb^{-1} , collected in proton-proton collisions at $\sqrt{s} = 13$ TeV in 2017–2018. To extract the values of ϕ_s and $\Delta\Gamma_s$, a time-dependent and flavor-tagged angular analysis of the $\mu^+ \mu^- K^+ K^-$ final state is performed. The analysis employs a dedicated tagging trigger and a novel opposite-side muon flavor tagger based on machine learning techniques. The measurement yields $\phi_s = -11 \pm 50$ (stat) ± 10 (syst) mrad and $\Delta\Gamma_s = 0.114 \pm 0.014$ (stat) ± 0.007 (syst) ps^{-1} , in agreement with the standard model predictions. When combined with the previous CMS measurement at $\sqrt{s} = 8$ TeV, the following values are obtained: $\phi_s = -21 \pm 44$ (stat) ± 10 (syst) mrad, $\Delta\Gamma_s = 0.1032 \pm 0.0095$ (stat) ± 0.0048 (syst) ps^{-1} , a significant improvement over the 8 TeV result.

"Published in Physics Letters B as doi:10.1016/j.physletb.2021.136188."

1 Introduction

Precision tests of the standard model (SM) of particle physics have become increasingly important, since no direct evidence for new physics has been found so far at the CERN LHC. Decays of B_s^0 mesons present important opportunities to probe the consistency of the SM. In this Letter, a new measurement of the CP -violating weak phase ϕ_s and the decay width difference $\Delta\Gamma_s$ between the light (B_s^L) and heavy (B_s^H) B_s^0 meson mass eigenstates is presented. Charge-conjugate states are implied throughout, unless stated otherwise.

The weak phase ϕ_s arises from the interference between direct B_s^0 meson decays to a CP eigenstate of $c\bar{c}s\bar{s}$ and decays through mixing to the same final state. In the SM, ϕ_s is related to the elements of the Cabibbo–Kobayashi–Maskawa matrix via $\phi_s \simeq -2\beta_s = -2 \arg(-V_{ts}V_{tb}^*/V_{cs}V_{cb}^*)$, neglecting penguin diagram contributions, where β_s is one of the angles of the unitary triangles. The current best determination of $-2\beta_s$ comes from a global fit to experimental data on b hadron and kaon decays. Assuming no physics beyond the SM (BSM) in the B_s^0 mixing and decays, a $-2\beta_s$ value of $-36.96^{+0.72}_{-0.84}$ mrad is determined [1]. New physics can modify this phase via the contribution of BSM particles to B_s^0 mixing [2, 3]. Since the numerical value of ϕ_s in the SM is known very precisely, even a small deviation from this value would constitute evidence of BSM physics. The decay width difference between the B_s^L and B_s^H eigenstates, on the other hand, is predicted less precisely at $\Delta\Gamma_s = 0.091 \pm 0.013 \text{ ps}^{-1}$ [4]. Its measurement provides an important test for theoretical predictions and can be used to further constrain new-physics effects [4].

The weak phase ϕ_s was first measured by the Fermilab Tevatron experiments [5–9], and then at the LHC by the ATLAS, CMS, and LHCb experiments [10–19], using $B_s^0 \rightarrow J/\psi \phi(1020)$ (referred to as $B_s^0 \rightarrow J/\psi \phi$ in what follows), $B_s^0 \rightarrow J/\psi f_0(980)$, and $B_s^0 \rightarrow J/\psi h^+h^-$ decays, where h stands for a kaon or pion. Measurements of ϕ_s in B_s^0 decays to $\psi(2S)\phi(1020)$ and $D_s^+D_s^-$ were performed by the LHCb Collaboration [20, 21].

In this Letter, CMS results on the $B_s^0 \rightarrow J/\psi \phi$ decay to the $\mu^+\mu^-K^+K^-$ final state are presented, and possible additional contributions to this final state from the $B_s^0 \rightarrow J/\psi f_0(980)$ and nonresonant $B_s^0 \rightarrow J/\psi K^+K^-$ decays are taken into account by including a term for an additional S -wave amplitude in the decay model. Compared to our previous measurement [14] at $\sqrt{s} = 8 \text{ TeV}$, we benefit from the increase in the center-of-mass energy from 8 to 13 TeV that nearly doubles the B_s^0 production cross section and a novel opposite-side (OS) muon flavor tagger. The new tagger employs machine learning techniques and achieves better discrimination power than previous methods. We also make use of a specialized trigger that requires an additional (third) muon, which can be used for flavor tagging, improving the tagging efficiency at the cost of a reduced number of signal events. As a result, the new measurement, while based on a similar number of B_s^0 candidates as the earlier one [14], allows us to double the precision in the determination of ϕ_s , as well as measure some of the parameters that were constrained to their world-average values in our previous work [14]. At the same time, the precision on parameters that do not benefit from the tagging information, such as $\Delta\Gamma_s$, is comparable to that in the previous measurement.

Final states that are mixtures of CP eigenstates require an angular analysis to separate the CP -odd and CP -even components. A time-dependent angular analysis can be performed by measuring the decay angles of the final-state particles and the proper decay length of the reconstructed B_s^0 candidate, which is equal to the proper decay time t multiplied by the speed of light, and referred to as ct in what follows.

In this measurement, we use the transversity basis [22] defined by the three decay angles

$\Theta = (\theta_T, \psi_T, \varphi_T)$, as illustrated in Fig. 1. The angles θ_T and φ_T are, respectively, the polar and azimuthal angles of the μ^+ in the rest frame of the J/ψ meson, where the x axis is defined by the direction of the ϕ meson momentum and the x - y plane is defined by the plane of the $\phi \rightarrow K^+K^-$ decay. The helicity angle ψ_T is the angle of the K^+ meson momentum in the ϕ meson rest frame with respect to the negative J/ψ meson momentum direction.

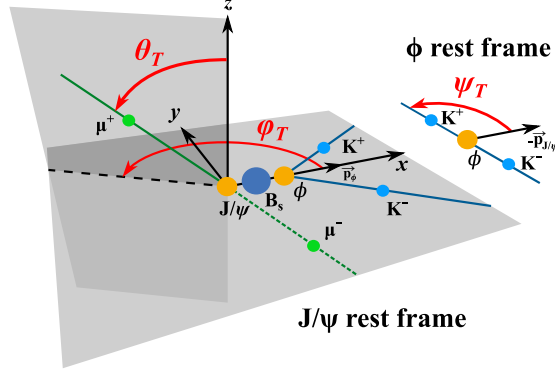


Figure 1: Definition of the three angles θ_T , ψ_T , and φ_T describing the topology of the $B_s^0 \rightarrow J/\psi \phi \rightarrow \mu^+ \mu^- K^+ K^-$ decay.

The differential decay rate of $B_s^0 \rightarrow J/\psi \phi \rightarrow \mu^+ \mu^- K^+ K^-$ is described by a function $\mathcal{F}(\Theta, ct, \alpha)$, as in Ref. [23]:

$$\frac{d^4\Gamma(B_s^0)}{d\Theta d(ct)} = \mathcal{F}(\Theta, ct, \alpha) \propto \sum_{i=1}^{10} O_i(ct, \alpha) g_i(\Theta), \quad (1)$$

where O_i are time-dependent functions, g_i are angular functions, and α is a set of physics parameters.

The functions $O_i(ct, \alpha)$ are:

$$O_i(ct, \alpha) = N_i e^{-\Gamma_s t} \left[a_i \cosh\left(\frac{\Delta\Gamma_s t}{2}\right) + b_i \sinh\left(\frac{\Delta\Gamma_s t}{2}\right) + c_i \cos(\Delta m_s t) + d_i \sin(\Delta m_s t) \right], \quad (2)$$

where Δm_s ($\Delta\Gamma_s$) is the absolute mass (decay width) difference between the B_s^L and B_s^H mass eigenstates, and Γ_s is the average decay width, defined as the arithmetic average of the B_s^L and B_s^H decay widths. The functions $g_i(\Theta)$ and the parameters N_i , a_i , b_i , c_i , and d_i are defined in Table 1.

Table 1: Angular and time-dependent terms of the signal model.

| i | $g_i(\theta_T, \psi_T, \varphi_T)$ | N_i | a_i | b_i | c_i | d_i |
|-----|--|------------------------------------|---|---|---|---|
| 1 | $2 \cos^2 \psi_T (1 - \sin^2 \theta_T \cos^2 \varphi_T)$ | $ A_0(0) ^2$ | 1 | D | C | $-S$ |
| 2 | $\sin^2 \psi_T (1 - \sin^2 \theta_T \sin^2 \varphi_T)$ | $ A_{\parallel}(0) ^2$ | 1 | D | C | $-S$ |
| 3 | $\sin^2 \psi_T \sin^2 \theta_T$ | $ A_{\perp}(0) ^2$ | 1 | $-D$ | C | S |
| 4 | $-\sin^2 \psi_T \sin 2\theta_T \sin \varphi_T$ | $ A_{\parallel}(0) A_{\perp}(0) $ | $C \sin(\delta_{\perp} - \delta_{\parallel})$ | $S \cos(\delta_{\perp} - \delta_{\parallel})$ | $\sin(\delta_{\perp} - \delta_{\parallel})$ | $D \cos(\delta_{\perp} - \delta_{\parallel})$ |
| 5 | $\frac{1}{\sqrt{2}} \sin 2\psi_T \sin^2 \theta_T \sin 2\varphi_T$ | $ A_0(0) A_{\parallel}(0) $ | $\cos(\delta_{\parallel} - \delta_0)$ | $D \cos(\delta_{\parallel} - \delta_0)$ | $C \cos(\delta_{\parallel} - \delta_0)$ | $-S \cos(\delta_{\parallel} - \delta_0)$ |
| 6 | $\frac{1}{\sqrt{2}} \sin 2\psi_T \sin 2\theta_T \cos \varphi_T$ | $ A_0(0) A_{\perp}(0) $ | $C \sin(\delta_{\perp} - \delta_0)$ | $S \cos(\delta_{\perp} - \delta_0)$ | $\sin(\delta_{\perp} - \delta_0)$ | $D \cos(\delta_{\perp} - \delta_0)$ |
| 7 | $\frac{2}{3}(1 - \sin^2 \theta_T \cos^2 \varphi_T)$ | $ A_S(0) ^2$ | 1 | $-D$ | C | S |
| 8 | $\frac{1}{3}\sqrt{6} \sin \psi_T \sin^2 \theta_T \sin 2\varphi_T$ | $ A_S(0) A_{\parallel}(0) $ | $C \cos(\delta_{\parallel} - \delta_S)$ | $S \sin(\delta_{\parallel} - \delta_S)$ | $\cos(\delta_{\parallel} - \delta_S)$ | $D \sin(\delta_{\parallel} - \delta_S)$ |
| 9 | $\frac{1}{3}\sqrt{6} \sin \psi_T \sin 2\theta_T \cos \varphi_T$ | $ A_S(0) A_{\perp}(0) $ | $\sin(\delta_{\perp} - \delta_S)$ | $-D \sin(\delta_{\perp} - \delta_S)$ | $C \sin(\delta_{\perp} - \delta_S)$ | $S \sin(\delta_{\perp} - \delta_S)$ |
| 10 | $\frac{4}{3}\sqrt{3} \cos \psi_T (1 - \sin^2 \theta_T \cos^2 \varphi_T)$ | $ A_S(0) A_0(0) $ | $C \cos(\delta_0 - \delta_S)$ | $S \sin(\delta_0 - \delta_S)$ | $\cos(\delta_0 - \delta_S)$ | $D \sin(\delta_0 - \delta_S)$ |

The coefficients C , S , and D contain the information about CP violation, and are defined as:

$$C = \frac{1 - |\lambda|^2}{1 + |\lambda|^2}, \quad S = -\frac{2|\lambda| \sin \phi_s}{1 + |\lambda|^2}, \quad D = -\frac{2|\lambda| \cos \phi_s}{1 + |\lambda|^2},$$

using the same sign convention as that in the LHCb measurement [16]. The amount of CP violation in the B_s^0 - \bar{B}_s^0 system is given by the complex parameter λ , defined as $\lambda = (q/p)(\bar{A}_f/A_f)$, where A_f (\bar{A}_f) is the decay amplitude of the B_s^0 (\bar{B}_s^0) meson to the final state f , and the parameters p and q relate the mass and flavor eigenstates through $B_s^H = p|B_s^0\rangle - q|\bar{B}_s^0\rangle$ and $B_s^L = p|B_s^0\rangle + q|\bar{B}_s^0\rangle$ [24]. The parameters $|A_\perp|^2$, $|A_0|^2$, and $|A_\parallel|^2$ are the magnitudes of the perpendicular, longitudinal, and parallel transversity amplitudes of the $B_s^0 \rightarrow J/\psi \phi$ decay, respectively; $|A_S|^2$ is the magnitude of the S -wave amplitude from $B_s^0 \rightarrow J/\psi f_0(980)$ and non-resonant $B_s^0 \rightarrow J/\psi K^+K^-$ decays, and the parameters δ_\perp , δ_0 , δ_\parallel , and δ_S are the respective strong phases.

Equation (1) represents the model for the B_s^0 meson decay, while the model for the \bar{B}_s^0 meson decay is obtained by changing the sign of the c_i and d_i terms in Eq. (2).

2 The CMS detector

The central feature of the CMS apparatus is a superconducting solenoid of 6 m internal diameter, providing a magnetic field of 3.8 T. Within the solenoid volume are a silicon pixel and strip tracker, a lead tungstate crystal electromagnetic calorimeter, and a brass and scintillator hadron calorimeter, each composed of a barrel and two endcap sections. Forward calorimeters extend the pseudorapidity (η) coverage provided by the barrel and endcap detectors. Muons are detected in gas-ionization chambers embedded in the steel flux-return yoke outside the solenoid.

The silicon tracker measures charged particles within the range $|\eta| < 2.5$. During the LHC running period when the data used in this Letter were recorded, the silicon tracker consisted of 1856 silicon pixel and 15 148 silicon strip detector modules.

Muons are measured in the range $|\eta| < 2.4$, with detection planes made using three technologies: drift tubes, cathode strip chambers, and resistive plate chambers. The efficiency to reconstruct and identify muons is greater than 96%. Matching muons to tracks measured in the silicon tracker results in a relative transverse momentum (p_T) resolution, for muons with p_T up to 100 GeV, of 1% in the barrel and 3% in the endcaps [25].

Events of interest are selected using a two-tiered trigger system [26]. The first level (L1), composed of custom hardware processors, uses information from the calorimeters and muon detectors to select events at a rate of around 100 kHz within a fixed time interval of less than 4 μ s. The second level, known as the high-level trigger (HLT), consists of a farm of processors running a version of the full event reconstruction software optimized for fast processing, and reduces the event rate to around 1 kHz before data storage.

A more detailed description of the CMS detector, together with a definition of the coordinate system used and the relevant kinematic variables, can be found in Ref. [27].

3 Event selection and simulated samples

The analysis is performed using data collected in proton-proton (pp) collisions at $\sqrt{s} = 13$ TeV during 2017–2018, corresponding to an integrated luminosity of 96.4 fb⁻¹. A trigger optimized

for the detection of b hadrons decaying to J/ψ mesons, along with an additional muon potentially usable for flavor tagging, is used to collect the data sample for the analysis. At L1, the trigger requires three muons, with the minimum p_T requirement on the highest p_T (leading, μ_1) and second-highest p_T (subleading, μ_2) muons of $p_T > 5$ and 3 GeV, respectively, and the dimuon invariant mass $m_{\mu_1\mu_2} < 9$ GeV. There is no p_T requirement on the third muon at L1. At the HLT, the three muons are required to be within the CMS geometrical acceptance $|\eta| < 2.5$; two of these muons must be oppositely charged, each have $p_T > 3.5$ GeV, form a J/ψ candidate with an invariant mass in the range 2.95–3.25 GeV, and have a probability to originate from a common vertex larger than 0.5%. The third muon is required to have $p_T > 2$ GeV and can be used to infer the flavor of the B_s^0 meson at production (i.e., its particle/antiparticle state), exploiting semileptonic $b \rightarrow \mu^- + X$ decays, as discussed further in Section 4.

Additional selection criteria are applied to events passing the HLT requirements. The numerical values of the selection cuts have been optimized with the help of the TMVA package [28, 29], using a genetic algorithm, to maximize the signal purity. First, J/ψ meson candidates are constructed using pairs of opposite-sign muons with $p_T > 3.5$ GeV and $|\eta| < 2.4$, and compatible with originating from a common vertex, obtained from a Kalman fit [30]. Candidates are accepted only if their invariant mass is within 150 MeV of the world-average J/ψ meson mass [31]. Next, pairs of opposite-sign tracks satisfying the high-purity requirement [32] with $p_T > 1.2$ GeV and $|\eta| < 2.5$, not associated with the muons that form the J/ψ candidate, are used to form ϕ candidates. The ϕ candidates are selected if the track pair has an invariant mass, assuming the kaon mass for both particles, within 10 MeV of the world-average ϕ meson mass [31]. Finally, the J/ψ and ϕ candidates are combined to form B_s^0 candidates: a common vertex (“ B_s^0 vertex”) is obtained from a fit with the four tracks, two for muons and two for kaons. The invariant mass of the B_s^0 candidate is obtained from a kinematic fit, where the invariant mass of the two muons is constrained to the world-average J/ψ meson mass [31]. The mass of the ϕ candidate is not constrained since its natural width exceeds the mass resolution.

Due to the high instantaneous luminosity of proton-proton collisions at the LHC, several primary vertices (PVs) are reconstructed in each event. The vertex that minimizes the angle between the B_s^0 candidate momentum vector and the line connecting this vertex with the B_s^0 decay vertex is chosen as the production vertex and is used to determine the characteristics of the B_s^0 candidate, such as proper decay length. We used simulations to study if the PV selection procedure introduces any bias in the measurement. It was found that in about 97% of the events, the selected PV is also the closest one to the point of origin of the B_s^0 meson. The impact of choosing a different vertex in the remaining cases on the final results is found to be negligible with respect to the total systematic uncertainties discussed in Section 6. The proper decay length is measured as $ct = cm_{B_s^0}^{\text{PDG}} L_{xy} / p_T$, where $m_{B_s^0}^{\text{PDG}}$ is the world-average B_s^0 mass [31] and L_{xy} is the reconstructed transverse decay length, which is defined as the distance in the transverse plane from the production vertex to the B_s^0 vertex. Additional selection criteria are applied to B_s^0 candidates, requiring $p_T > 11$ GeV, the four-track vertex fit χ^2 probability $> 2\%$, an invariant mass in the 5.24–5.49 GeV range, and a proper decay length $ct > 70 \mu\text{m}$, with an uncertainty $\sigma_{ct} < 50 \mu\text{m}$. The proper decay length uncertainty is obtained by propagating the uncertainties in the decay distance and the p_T of the B_s^0 candidate to ct . In about 2% of the events more than one B_s^0 candidate is selected. In these cases, the candidate with the highest vertex fit probability is chosen. The impact of this choice on the measurement has been evaluated by redoing the analysis using the candidate with the lowest vertex fit probability. No sizable bias has been observed with respect to the total systematic uncertainties discussed in Section 6. A total of 65 500 $B_s^0 \rightarrow J/\psi \phi$ candidates are selected.

Simulated event samples are used to measure the selection efficiency and the flavor tagging performance. These samples are produced using the PYTHIA 8.230 Monte Carlo (MC) event generator [33] with the underlying event tune CP5 [34] and the parton distribution function set NNPDF3.1 [35]. The b hadron decays are modeled with the EVTGEN 1.6.0 package [36]. Final-state photon radiation is accounted for in the EVTGEN simulation with PHOTOS 215.5 [37, 38]. The response of the CMS detector is simulated using the GEANT4 package [39]. The effect of multiple collisions in the same or neighboring bunch crossings (pileup) is accounted for by overlaying simulated minimum bias events on the hard-scattering process. Simulated samples are then reconstructed using the same software as for collision data.

The simulation is validated via comparison with background-subtracted data in a number of control distributions. The B_s^0 candidate invariant mass distribution after the signal selection is shown in Fig. 2, whereas the proper decay length and its uncertainty distributions are shown in Fig. 3.

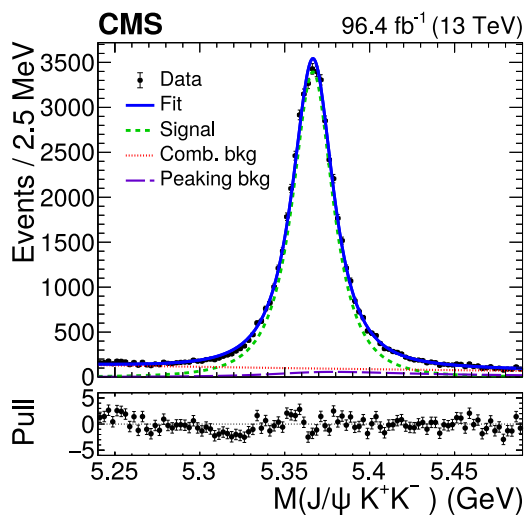


Figure 2: The invariant mass distribution of the $B_s^0 \rightarrow J/\psi \phi \rightarrow \mu^+ \mu^- K^+ K^-$ candidates in data. The vertical bars on the points represent the statistical uncertainties. The solid line represents a projection of the fit to data (as discussed in Section 5, solid markers), the dashed line corresponds to the signal, the dotted line to the combinatorial background, and the long-dashed line to the peaking background from $B^0 \rightarrow J/\psi K^*(892)^0 \rightarrow \mu^+ \mu^- K^+ \pi^-$, as obtained from the fit. The distribution of the differences between the data and the fit, divided by the combined uncertainty in the data and the best fit function for each bin (pulls) is displayed in the lower panel.

4 Flavor tagging

The flavor of the B_s^0 candidate at production is determined with an OS flavor tagging algorithm. The OS approach is based on the fact that b quarks are predominantly produced in $b\bar{b}$ pairs, and therefore one can infer the initial B_s^0 meson flavor by determining the flavor of the other (“OS”) b quark in the event.

In this analysis, the flavor of the OS b hadron is deduced by exploiting the semileptonic $b \rightarrow \mu^- + X$ decay, where the muon sign ζ is used as the tagging variable ($\zeta = -1$ for B_s^0). This technique works on a probabilistic basis. If no OS muon is found, the event is considered as untagged ($\zeta = 0$). The tagging efficiency ε_{tag} is defined as the fraction of candidate events that

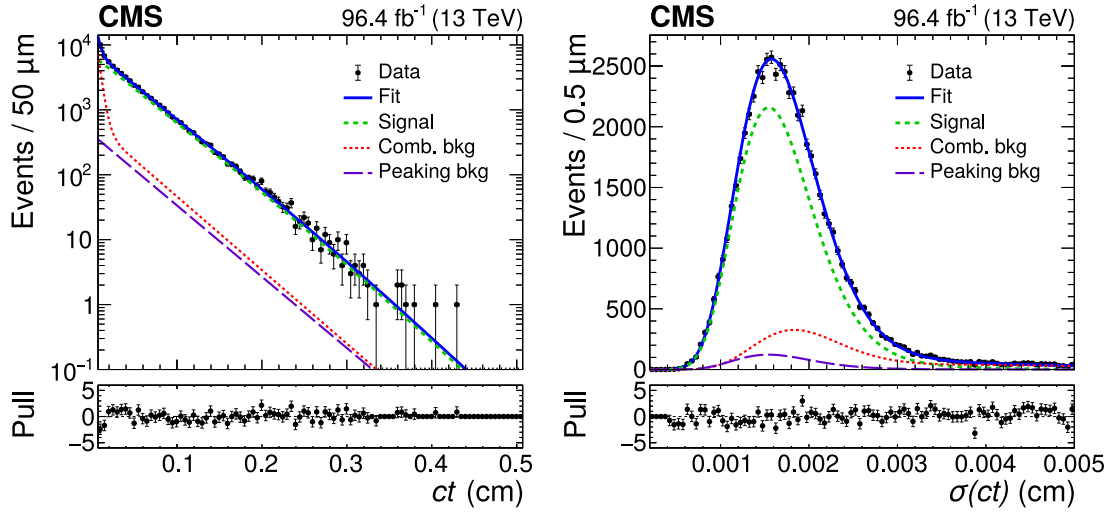


Figure 3: The ct distribution (left) and its uncertainty (right) for the $B_s^0 \rightarrow J/\psi \phi \rightarrow \mu^+ \mu^- K^+ K^-$ candidates in data. The notations are as in Fig. 2.

are tagged. When a muon is found, the tag is defined to be correct (“right tag”) if the flavor predicted using the muon sign and the actual B_s^0 meson flavor at production coincide. The correlation between the muon sign and the signal B_s^0 meson flavor is diluted by wrong tags (mistags) originating from cascade $b \rightarrow c \rightarrow \mu^+ + X$ decays, oscillation of the OS B^0 or B_s^0 meson, and muons originating from other sources, such as J/ψ meson and charged pion and kaon decays. The mistag fraction ω_{tag} is defined as the ratio between the number of wrongly tagged events and the total number of tagged events. It is used to compute the dilution $\mathcal{D} \equiv 1 - 2\omega_{\text{tag}}$, which is a measure of the performance degradation due to mistagged events. The tagging power $P_{\text{tag}} \equiv \varepsilon_{\text{tag}} \mathcal{D}^2$ is the effective tagging efficiency, which takes into account the dilution and is used as a figure of merit in maximizing the algorithm performance.

To maximize the sensitivity of this measurement, we have developed a novel OS muon tagger taking advantage of machine learning techniques. The use of deep neural networks (DNNs) in the new tagger leads to lowering of the mistag probability ω_{tag} and reducing of the related systematic uncertainties. The use of a dedicated trigger, which requires an OS muon, dramatically increases the fraction of tagged candidates compared to our earlier measurement [14]. Taken together, these two improvements increase the muon tagging performance by $\approx 20\%$ compared to that in Ref. [14].

For each event, we search for a candidate OS muon consistent with originating from the same production vertex as the signal B_s^0 meson. This *tagging* muon is required to have $p_T > 2 \text{ GeV}$, $|\eta| < 2.4$, the longitudinal impact parameter with respect to the production vertex $IP_z < 1.0 \text{ cm}$, and the distance from the B_s^0 candidate momenta in the (η, ϕ) plane $\Delta R_{\eta, \phi} > 0.4$. Tracks that belong to the reconstructed $B_s^0 \rightarrow J/\psi \phi \rightarrow \mu^+ \mu^- K^+ K^-$ decay are explicitly excluded from consideration. In order to reduce the contamination from light-flavor hadrons misreconstructed as tagging muons, a discriminator based on a DNN was developed using the KERAS library [40] within the TMVA toolkit. This discriminator, called the “DNN against light hadrons” in the following, uses 25 input features related to the muon kinematics and reconstruction quality, and is trained with 3.5×10^6 simulated muon candidates of which 2.5×10^5 are misreconstructed hadrons. The following DNN hyperparameters are optimized through a grid scan to maximize the discrimination power: number of layers, number of neurons for each layer, and the dropout probability. No signs of overtraining are observed at the chosen hyperparameters configura-

tion when comparing the output distributions from the testing and training samples. Tagging muons are required to pass a working point of the DNN output that has an efficiency of $\approx 98\%$ for genuine muons and $\approx 33\%$ for misreconstructed light-flavor hadrons, when evaluated using muon candidates reconstructed with the CMS particle-flow (PF) algorithm [41]. In $\approx 3\%$ of the events where more than one tagging muon candidate passes all the above selections, only the highest p_T one is kept.

Another DNN is used to further discriminate the right- and wrong-tag muons, as well as to predict the mistag probability on a per-event basis. This DNN, referred to as the muon tagger DNN, has been developed using the KERAS library within the TMVA toolkit, based on simulated $B_s^0 \rightarrow J/\psi \phi \rightarrow \mu^+ \mu^- K^+ K^-$ events, and calibrated with self-tagging $B^\pm \rightarrow J/\psi K^\pm$ MC and data samples, as described below.

The input features of the muon tagger DNN are of two kinds: muon variables and cone variables. The muon variables are the muon p_T , η , transverse and longitudinal impact parameters with respect to the production vertex, along with their uncertainties, the distance $\Delta R_{\eta,\phi}$ to the signal B_s^0 candidate, and the discriminant of the DNN against light hadrons. The cone variables are related to the activity in a cone of radius $\Delta R_{\eta,\phi} = 0.4$ around the muon momentum direction and include the relative PF isolation [41], the scalar p_T sum of all additional tracks within the cone, the sum of their charges weighted by the track p_T , the muon relative momentum and $\Delta R_{\eta,\phi}$ with respect to the vector sum of the momenta of all additional tracks within the cone, and the ratio of the energy of the muon to the total energy of all additional tracks within the cone (assuming the pion mass for each track). The muon tagger DNN is trained on 2.8×10^5 simulated $B_s^0 \rightarrow J/\psi \phi$ events, of which about 85 000 have a wrong tag. Its structure is optimized similarly to that for the DNN against light hadrons. The optimal DNN has three dense layers of 200 neurons, each with a rectified linear unit activation function. A dropout layer with a dropout probability of 40% is placed after each dense layer. The cross-entropy loss function and the Adam optimizer [42] are used. The DNN is constructed in such a way that its output score d is equal to the probability of tagging the event correctly. Therefore, the per-event mistag probability is simply $\omega_{\text{evt}} = 1 - d$.

The output d of the tagger is calibrated using a self-tagging data sample of $B^\pm \rightarrow J/\psi K^\pm \rightarrow \mu^+ \mu^- K^\pm$ events, where the charge of the kaon corresponds to the charge and flavor of the B^\pm meson. The same trigger and J/ψ candidate reconstruction requirements as for the B_s^0 signal sample are applied. A charged particle with $p_T > 1.6$ GeV, assumed to be a kaon, is combined in a kinematic fit with the dimuon pair to form the B^\pm candidate. The calibration is performed separately for the 2017 and 2018 data samples, by comparing the measured mistag fraction (ω_{meas}) with the ω_{evt} predicted by the muon tagger DNN. The B^\pm events are divided into 100 bins in ω_{evt} and the right- and wrong-tag events are separately counted in each bin to extract the corresponding ω_{meas} value. The B^\pm signal in each bin is discriminated from the background via a binned likelihood fit to the $J/\psi K^\pm$ invariant mass distribution in the 5.10–5.65 GeV range.

The calibration results for the 2017 and 2018 B^\pm data are shown in Fig. 4. The data points are fitted with a linear function $a + b\omega_{\text{evt}}$. The calibration parameters returned by the fit for the 2017 (2018) data samples are $a = -0.0010 \pm 0.0040$, $b = 1.012 \pm 0.013$ ($a = 0.0031 \pm 0.0031$, $b = 1.011 \pm 0.010$), statistically compatible with a unit slope and zero offset.

The calibration of the DNN output is also verified with a procedure similar to that described above using an independent sample of simulated $B_s^0 \rightarrow J/\psi \phi$ and $B^\pm \rightarrow J/\psi K^\pm$ events. The reconstructed B_s^0 and B^\pm mesons are matched to the generated ones in order to find their true flavor at production. In general, the measured mistag probability is predicted very accurately by ω_{evt} over the entire measured range for all the examined samples and processes, with more

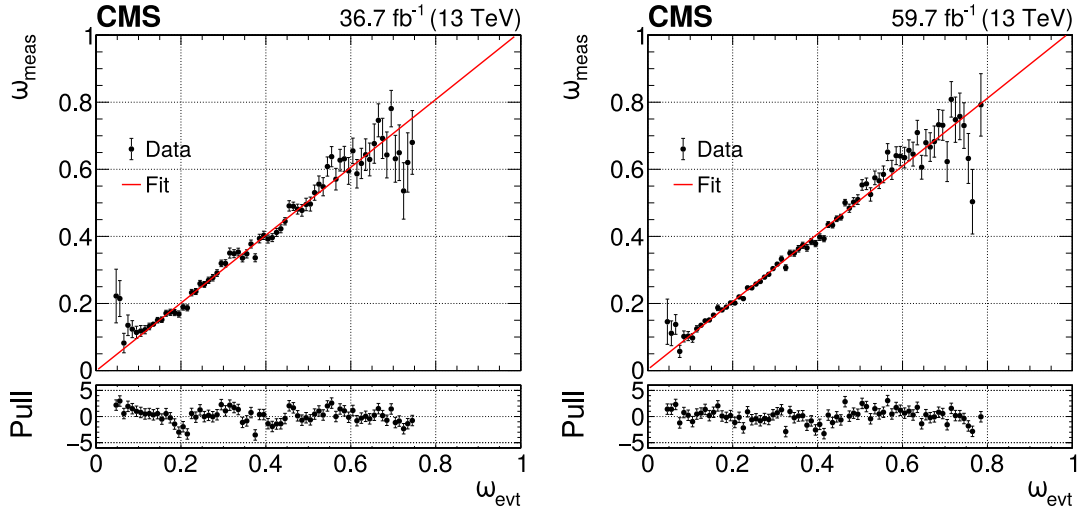


Figure 4: Results of the calibration of the per-event mistag probability ω_{evt} based on $B^\pm \rightarrow J/\psi K^\pm \rightarrow \mu^+ \mu^- K^\pm$ decays from the 2017 (left) and 2018 (right) data samples. The vertical bars represent the statistical uncertainties. The solid line shows a linear fit to data (solid markers). The pull distributions between the data and the fit function in each bin are shown in the lower panels.

than 90% of the tagged events falling in the $\omega_{\text{evt}} = 0.1\text{--}0.5$ range in all cases. Residual differences are well approximated by linear functions with slopes close to unity and offsets consistent with zero. The χ^2 per degree of freedom values for all fits are below 2. We conclude that the value of ω_{evt} returned by the tagging DNN is a good approximation of the true mistag probability in data, with minor residual differences taken into account with calibration functions.

The calibrated flavor tagger performance, evaluated using $B^\pm \rightarrow J/\psi K^\pm$ events in data, is shown in Table 2. A tagging efficiency of $\approx 50\%$ and a tagging power of $\approx 10\%$ are achieved in both the 2017 and 2018 data samples. The efficiency is much higher than the semileptonic b hadron branching fraction due to the requirement of an additional OS muon at the HLT, as described in Section 3.

Possible differences in the mistag probability calibration between the B_s^0 and B^\pm samples, as well as the statistical uncertainties in the calibration parameters and possible variations from linearity of the calibration function, are considered as systematic uncertainties and described in Section 6.

Table 2: Calibrated opposite-side muon tagger performance evaluated using $B^\pm \rightarrow J/\psi K^\pm$ events in the 2017 and 2018 data samples. The uncertainties shown are statistical only.

| Data sample | ϵ_{tag} (%) | ω_{tag} (%) | P_{tag} (%) |
|-------------|-----------------------------|---------------------------|----------------------|
| 2017 | 45.7 ± 0.1 | 27.1 ± 0.1 | 9.6 ± 0.1 |
| 2018 | 50.9 ± 0.1 | 27.3 ± 0.1 | 10.5 ± 0.1 |

5 Maximum-likelihood fit

An unbinned multidimensional extended maximum-likelihood fit is performed on the combined data samples using 8 observables as input: the B_s^0 candidate invariant mass $m_{B_s^0}$, the three decay angles Θ of the reconstructed B_s^0 candidate, the flavor tag decision ξ , the mistag fraction ω_{evt} , the proper decay length of the B_s^0 candidate ct , and its uncertainty σ_{ct} .

From the multidimensional fit, the physics parameters of interest ϕ_s , $\Delta\Gamma_s$, Γ_s , Δm_s , $|\lambda|$, the squares of amplitudes $|A_\perp|^2$, $|A_0|^2$, $|A_S|^2$, and the strong phases δ_\parallel , δ_\perp , and $\delta_{S\perp}$ are determined, where $\delta_{S\perp}$ is defined as the difference $\delta_S - \delta_\perp$. The $B_s^0 \rightarrow J/\psi \phi$ amplitudes are normalized to unity by constraining $|A_\parallel|^2$ to $1 - |A_\perp|^2 - |A_0|^2$. The fit model is validated with simulated pseudo-experiments and with simulated samples with different input parameter sets.

The likelihood function is composed of the probability density functions (pdfs) describing the signal and background components. The likelihood fit algorithm is implemented using the ROOFIT package [28, 43]. The signal and background pdfs are formed as the product of functions that model the invariant mass distribution and the time-dependent decay rates of the reconstructed candidates. In addition, the signal pdf includes the efficiency functions. The event pdf P is defined as:

$$P = \frac{N_{\text{sig}}}{N_{\text{tot}}} P_{\text{sig}} + \frac{N_{\text{bkg}}}{N_{\text{tot}}} P_{\text{bkg}}, \quad (3)$$

where

$$P_{\text{sig}} = \varepsilon(ct) \varepsilon(\Theta) [\tilde{\mathcal{F}}(\Theta, ct, \alpha) \otimes G(ct, \sigma_{ct})] P_{\text{sig}}(m_{B_s^0}) P_{\text{sig}}(\sigma_{ct}) P_{\text{sig}}(\xi) \quad (4)$$

and

$$P_{\text{bkg}} = P_{\text{bkg}}(\cos \theta_T, \phi_T) P_{\text{bkg}}(\cos \psi_T) P_{\text{bkg}}(ct) P_{\text{bkg}}(m_{B_s^0}) P_{\text{bkg}}(\sigma_{ct}) P_{\text{bkg}}(\xi). \quad (5)$$

The corresponding negative log likelihood is:

$$-\ln \mathcal{L} = -\sum_{i=0}^{N_{\text{evt}}} \ln P_i + N_{\text{tot}} - N_{\text{evt}} \ln N_{\text{tot}}. \quad (6)$$

Here, P_{sig} and P_{bkg} are the pdfs that describe the $B_s^0 \rightarrow J/\psi \phi \rightarrow \mu^+ \mu^- K^+ K^-$ signal and background contributions, respectively. The yields of signal and background events are N_{sig} and N_{bkg} , respectively, N_{tot} is their sum, and $N_{\text{evt}} = 65500$ is the number of candidates selected in data. The pdf $\tilde{\mathcal{F}}(\Theta, ct, \alpha)$ is the differential decay rate function $\mathcal{F}(\Theta, ct, \alpha)$ defined in Eq. (1), modified to include the flavor information ξ and the dilution term $(1 - 2\omega_{\text{evt}})$, which are applied as multiplicative factors to each of the c_i and d_i terms in Eq. (2). In the $\tilde{\mathcal{F}}$ expression, the value of δ_0 is set to zero, following a general convention [6, 8], and the value of $\Delta\Gamma_s$ is constrained to be positive, based on the LHCb measurement [44]. All the parameters of the pdfs are allowed to float in the final fit, unless explicitly stated otherwise.

The functions $\varepsilon(ct)$ and $\varepsilon(\Theta)$ model the dependence of the signal reconstruction efficiency on the proper decay length and the three angles of the transversity basis, respectively. The proper decay length efficiency is parameterized with a fourth-order Chebyshev polynomial multiplied by an exponential function with a negative slope, while the angular efficiency is parameterized with spherical harmonics and Legendre polynomials up to order six. Both parameterizations are obtained from fits to the respective efficiency histograms in $B_s^0 \rightarrow J/\psi \phi$ simulated events, and are fixed in the fit to data.

The term $G(ct, \sigma_{ct})$ is a Gaussian resolution function, which makes use of the per-event decay length uncertainty σ_{ct} , scaled by a correction factor κ introduced to account for the residual effects when the decay length uncertainty is used to model the ct resolution. The value of κ is estimated using simulated samples and is equal to ≈ 1.2 for both the 2017 and 2018 data samples.

The signal mass pdf $P_{\text{sig}}(m_{B_s^0})$ is a Johnson's S_U distribution [45], while the decay length uncertainty pdf $P_{\text{sig}}(\sigma_{ct})$ is described by the sum of two Gamma distributions. These pdfs best model each individual variable in one-dimensional fits to simulated samples.

The background pdf contains two terms to model both the combinatorial background and the peaking background, dominated by $B^0 \rightarrow J/\psi K^*(892)^0 \rightarrow \mu^+ \mu^- K^+ \pi^-$, where the pion is assumed to be a kaon candidate. The background from $\Lambda_b^0 \rightarrow J/\psi p K^- \rightarrow \mu^+ \mu^- p K^-$, where the proton is assumed to be a kaon candidate, is estimated using simulated events to have a negligible effect on the fit results compared to the systematic uncertainties discussed in Section 6. The background invariant mass pdf $P_{\text{bkg}}(m_{B_s^0})$ is described by an exponential function for the combinatorial background and a Johnson's S_U distribution for the peaking background. The background decay length pdf $P_{\text{bkg}}(ct)$ is described by the sum of two exponential distributions for the combinatorial background, while a single exponential distribution is used for the peaking background. The angular parts of the background pdfs $P_{\text{bkg}}(\cos \theta_T, \varphi_T)$ and $P_{\text{bkg}}(\cos \psi_T)$ are described analytically by a series of Legendre polynomials for $\cos \theta_T$ and $\cos \psi_T$, and sinusoidal functions for φ_T . For the $\cos \theta_T$ and φ_T variables, a two-dimensional pdf is used to take into account a possible correlation between the two. The background decay length uncertainty pdf $P_{\text{bkg}}(\sigma_{ct})$ is described by a sum of two Gamma distributions for the combinatorial background, while the peaking background is fixed to that for the signal.

The tag pdfs are defined as $P(\zeta) = 1 - \varepsilon_{\text{tag}}$ for the untagged events ($\zeta = 0$) and $P(\zeta) = \varepsilon_{\text{tag}}(1 \pm A_{\text{tag}})/2$ for the tagged ones ($\zeta = \pm 1$), where ε_{tag} is the tagging efficiency and A_{tag} is the tagging asymmetry, defined as the difference between the numbers of positively and negatively tagged events ($\zeta = \pm 1$) divided by the total number. The measured tagging asymmetry is found to be compatible with zero.

The correlation between the different fit components has been studied in both data and simulations, and found to be negligible.

The peaking background part of P_{bkg} is determined using simulated samples, while the initial combinatorial background part is found from a fit to the B_s^0 invariant mass sidebands 5.24–5.28 GeV and 5.45–5.49 GeV in data, and then left free to float in the final fit, starting from this initial pdf. The signal and background components of the decay length uncertainty pdf are fixed to the ones obtained from a two-dimensional fit together with the invariant mass pdf. The 2017 and 2018 data samples are fitted simultaneously. The joint likelihood function of the simultaneous fit shares the decay rate model, the invariant mass pdfs, the peaking background model, and the lifetime and angular components of the combinatorial background model between the two samples. The number of signal and background events are measured separately in each data sample, as is the tagging efficiency. The efficiency functions, $P(\sigma_{ct})$ pdfs, tag pdfs, and κ factors are also specific to each data sample.

6 Systematic uncertainties and results

The results of the fit with their statistical and systematic uncertainties are given in Table 3, whereas the statistical correlations between the measured parameters are reported in Appendix A. Statistical uncertainties are obtained from the increase in $-\log \mathcal{L}$ by 0.5, whereas systematic uncertainties are described below and summarized in Table 4. The measured number of $B_s^0 \rightarrow J/\psi \phi \rightarrow \mu^+ \mu^- K^+ K^-$ signal events from the fit is $48\,500 \pm 250$. The distributions of the input observables and the corresponding fit projections are shown in Figs. 2, 3, and 5.

Several sources of systematic uncertainties in the physics parameters are studied by testing the various assumptions made in the fit model and those associated with the fitting procedure.

Model bias: Possible biases in the fitting procedure are evaluated by generating 1000 pseudo-experiments, each statistically equivalent to the data samples, from the fitted model in data

Table 3: Results of the fit to data. Statistical uncertainties are obtained from the increase in $-\log \mathcal{L}$ by 0.5, whereas systematic uncertainties are described below and summarized in Table 4.

| Parameter | Fit value | Stat. uncer. | Syst. uncer. |
|---|-----------|----------------------|--------------|
| ϕ_s [mrad] | -11 | ± 50 | ± 10 |
| $\Delta\Gamma_s$ [ps^{-1}] | 0.114 | ± 0.014 | ± 0.007 |
| Δm_s [$\hbar \text{ps}^{-1}$] | 17.51 | $^{+0.10}_{-0.09}$ | ± 0.03 |
| $ \lambda $ | 0.972 | ± 0.026 | ± 0.008 |
| Γ_s [ps^{-1}] | 0.6531 | ± 0.0042 | ± 0.0026 |
| $ A_0 ^2$ | 0.5350 | ± 0.0047 | ± 0.0049 |
| $ A_\perp ^2$ | 0.2337 | ± 0.0063 | ± 0.0045 |
| $ A_S ^2$ | 0.022 | $^{+0.008}_{-0.007}$ | ± 0.016 |
| δ_\parallel [rad] | 3.18 | ± 0.12 | ± 0.03 |
| δ_\perp [rad] | 2.77 | ± 0.16 | ± 0.05 |
| $\delta_{S\perp}$ [rad] | 0.221 | $^{+0.083}_{-0.070}$ | ± 0.048 |

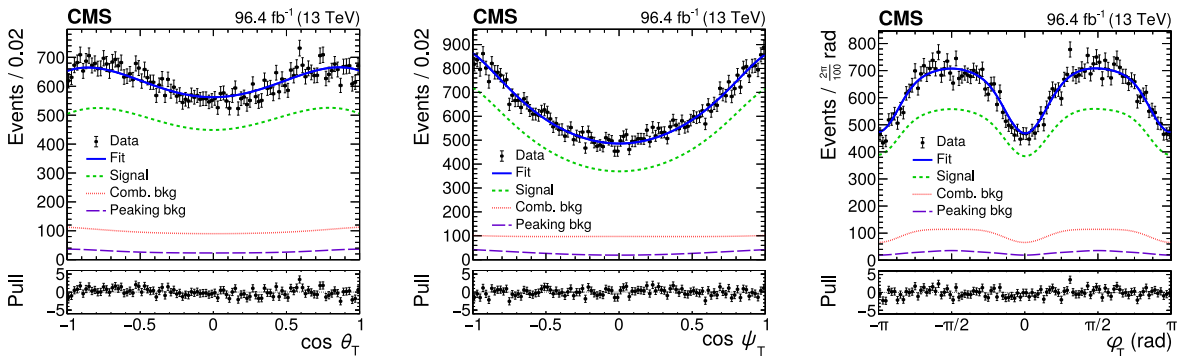


Figure 5: The angular distributions $\cos \theta_T$ (left), $\cos \psi_T$ (middle), and φ_T (right) for the B_s^0 candidates and the projections from the fit. The notations are as in Fig. 2.

(referred to as “nominal-model pseudo-experiments” in what follows). Each of them is fitted with the nominal model, and the pull distributions (i.e., the difference divided by the combined uncertainty) between the parameters obtained from the fit and their input values are produced. Each pull distribution is fitted with a Gaussian function, and the estimated central value is taken as the corresponding systematic uncertainty, if different from zero by more than its error. To avoid double-counting this uncertainty, whenever pseudo-experiments are used to evaluate other systematic uncertainties, the model bias is always subtracted. In these cases, the corresponding pull distributions are compared to those obtained with the nominal-model pseudo-experiments. If the mean of the pull distribution differs from the mean of the nominal-model distribution by more than their combined RMS, the difference is taken as the corresponding systematic uncertainty.

Model assumptions: The assumptions made in defining the likelihood functions are tested by generating pseudo-experiments with different hypotheses and fitting the samples with the nominal model. The following assumptions are tested: signal and background invariant mass models, background proper decay length model, and background angular model. Pull distributions with respect to the input values are used to evaluate the systematic uncertainty, as described in the “model bias” paragraph.

Angular efficiency: The systematic uncertainty related to the limited MC event count used to estimate the angular efficiency function is evaluated by regenerating the efficiency histograms

Table 4: Summary of the systematic uncertainties. The dashes (—) mean that the corresponding uncertainty is not applicable. The total systematic uncertainty is obtained as the quadratic sum of the individual contributions.

| | ϕ_s [mrad] | $\Delta\Gamma_s$ [ps ⁻¹] | Δm_s [\hbar ps ⁻¹] | $ \lambda $ | Γ_s [ps ⁻¹] | $ A_0 ^2$ | $ A_\perp ^2$ | $ A_S ^2$ | δ_\parallel [rad] | δ_\perp [rad] | $\delta_{S\perp}$ [rad] |
|--|--------------------|---|--|-------------|-----------------------------------|-----------|---------------|------------|-----------------------------|-------------------------|----------------------------|
| Statistical uncertainty | 50 | 0.014 | 0.10 | 0.026 | 0.0042 | 0.0047 | 0.0063 | 0.0077 | 0.12 | 0.16 | 0.083 |
| Model bias | 7.9 | 0.0019 | — | 0.0035 | 0.0005 | 0.0002 | 0.0012 | 0.001 | 0.020 | 0.016 | 0.006 |
| Model assumptions | — | — | — | 0.0046 | 0.0003 | — | 0.0013 | 0.001 | 0.017 | 0.019 | 0.011 |
| Angular efficiency | 3.8 | 0.0006 | 0.007 | 0.0057 | 0.0002 | 0.0008 | 0.0010 | 0.002 | 0.006 | 0.015 | 0.015 |
| Proper decay length efficiency | 0.3 | 0.0062 | 0.001 | 0.0002 | 0.0022 | 0.0014 | 0.0023 | 0.001 | 0.001 | 0.002 | 0.002 |
| Proper decay length resolution | 3.5 | 0.0009 | 0.021 | 0.0015 | 0.0006 | 0.0007 | 0.0009 | 0.007 | 0.006 | 0.025 | 0.022 |
| Data/simulation difference | 0.6 | 0.0008 | 0.004 | 0.0003 | 0.0003 | 0.0044 | 0.0029 | 0.007 | 0.007 | 0.007 | 0.028 |
| Flavor tagging | 0.5 | $<10^{-4}$ | 0.006 | 0.0002 | $<10^{-4}$ | 0.0003 | $<10^{-4}$ | $<10^{-3}$ | 0.001 | 0.007 | 0.001 |
| Sig./bkg. ω_{evt} difference | 3.0 | — | — | — | 0.0005 | — | 0.0008 | — | — | — | 0.006 |
| Peaking background | 0.3 | 0.0008 | 0.011 | $<10^{-4}$ | 0.0002 | 0.0005 | 0.0002 | 0.003 | 0.005 | 0.007 | 0.011 |
| S-P wave interference | — | 0.0010 | 0.019 | — | 0.0005 | 0.0005 | — | 0.013 | — | 0.019 | 0.019 |
| $P(\sigma_{ct})$ uncertainty | $<10^{-1}$ | 0.0019 | 0.028 | 0.0004 | 0.0008 | 0.0006 | 0.0008 | 0.001 | 0.001 | 0.002 | 0.005 |
| Total systematic uncertainty | 10.0 | 0.0070 | 0.032 | 0.0083 | 0.0026 | 0.0049 | 0.0045 | 0.016 | 0.028 | 0.045 | 0.048 |

1000 times using the reference one, with the fit repeated after reestimating the efficiency. The root mean square (RMS) of the obtained physics parameter distributions is taken as the systematic uncertainty.

Proper decay length efficiency: The proper decay length efficiency is first validated by fitting the B^\pm proper decay length distribution in the control $B^\pm \rightarrow J/\psi K^\pm$ channel, using several different data-taking periods. Each fit is performed applying the efficiency function evaluated using simulated $B^\pm \rightarrow J/\psi K^\pm$ samples with the same procedure used for the $B_s^0 \rightarrow J/\psi \phi$ analysis. We consider eight different data-taking periods, each with the number of B^\pm candidates comparable with the number of signal candidates in the B_s^0 sample used in the analysis. We also consider the 2017 and 2018 data-taking periods as two additional large control data sets. The results are in good agreement with the world-average B^\pm meson lifetime [31], with differences no larger than 1.5 standard deviations, showing no bias or instabilities during the data taking. Having verified that the efficiency parameterization does not introduce any noticeable bias, we evaluate the related systematic uncertainty by varying the parameters of the proper decay length efficiency function within their statistical uncertainties. The RMS of the distribution of each extracted physics parameter of interest with respect to the nominal fit value is taken as the corresponding systematic uncertainty. We assign a systematic uncertainty to the efficiency model by repeating the fit using the efficiency histogram instead of a smooth efficiency function, and taking the difference from the nominal result as the uncertainty.

Proper decay length resolution: A systematic uncertainty is assigned to the proper decay length resolution by varying the κ correction factor by $\pm 10\%$, as estimated from a data-to-simulation comparison, repeating the fit, and taking the largest difference from the nominal result as the uncertainty. We also evaluate a systematic uncertainty related to the assumption that κ is independent of the proper decay length, by parametrizing κ as a function of ct using simulated samples. A systematic uncertainty is assigned with the same methodology used to evaluate the “model assumption” systematic uncertainties, using the $\kappa(ct)$ parametrization as an alternative hypothesis.

Data/simulation difference: The efficiency parametrization is found to be very sensitive to the muon and kaon p_T , and B_s^0 meson rapidity distributions, hence a systematic uncertainty is assigned to cover the differences in each of these variables, between data and simulation. The effect is evaluated by reweighting the simulated distributions in each variable to agree with the data. The same weights are applied to the simulated samples used to estimate the efficiencies,

which are then recomputed. The fit is repeated in each case and the sum in quadrature of the differences from the nominal result is taken as the systematic uncertainty.

Flavor tagging: The uncertainties associated with the flavor tagging are propagated by varying the parameters of the mistag probability calibration curves within their statistical uncertainties. For each variation, new calibration curves are produced and the data are refitted. The RMS of each fitted parameter distribution is then taken as the corresponding systematic uncertainty. We also evaluate the effect of the assumption that the signal and calibration channels have the same mistag calibration. The difference between the B_s^0 and B^\pm calibrations is evaluated using simulated samples and is taken as the systematic uncertainty. The effect of the calibration function shape is evaluated by repeating the fit using a third-order polynomial and taking the difference with respect to the nominal result as the systematic uncertainty. The combined contribution of the three sources to the total systematic uncertainty is negligible.

Different ω_{evt} distribution in signal and background: A systematic uncertainty is assigned to the possible differences in the mistag probabilities between signal and background. The separate signal and background ω_{evt} distributions in data are first measured by using the B_s^0 candidate invariant mass signal and sidebands regions. These distributions are separately modeled using the Kernel Density Estimation method [46, 47] and added to the fitting model. One thousand pseudo-experiments are generated and pull distributions with respect to the input values are used to evaluate the systematic uncertainty, as described in the “model bias” paragraph.

Peaking background: The systematic uncertainty related to the fixed yield of the peaking background component is evaluated by repeating the fit using a different yield obtained from a $B^0 \rightarrow J/\psi K^*(892)^0$ control sample in data. The difference with respect to the nominal result is taken as the systematic uncertainty. A systematic uncertainty is also assigned to the proper decay length modeling of the peaking background by forcing the lifetime to match the world-average value [31], repeating the fit, and taking the difference from the nominal result as the systematic uncertainty.

S-P wave interference: The fit model does not take into account the difference in the invariant mass dependence between the P -wave from the $B_s^0 \rightarrow J/\psi \phi$ decay and the S -wave, which modifies their interference by a factor k_{SP} . The corresponding systematic uncertainty is estimated using pseudo-experiments. The k_{SP} factor is computed by integrating the P - and S -wave interference term in the ϕ candidate mass range, assuming that the P -wave amplitude is described by a relativistic Breit–Wigner distribution and the S -wave amplitude by a constant, and found to be $k_{\text{SP}} = 0.54$. Different S -wave lineshapes are found to lead to very similar values of k_{SP} , with a variation no larger than $\approx 2\%$. One thousand pseudo-experiments are generated applying $k_{\text{SP}} = 0.54$ to the $i = 8, 9, 10$ terms in Table 1 related to the S - and P -wave interference. Pull distributions with respect to the input values are used to evaluate the systematic uncertainty, as described in the “model bias” paragraph. The parameters $|A_S|^2$ and Δm_s are the only ones whose total uncertainty is affected significantly by this approximation.

$P(\sigma_{ct})$ uncertainty: In the fit to data the proper decay length uncertainty pdf is fixed to the one obtained from a pre-fit, as described in Section 5. A systematic uncertainty is assigned by sampling this distribution 1000 times, using the parameter uncertainties obtained from the pre-fit. Each time the fit to data is repeated and the standard deviation of the obtained physics parameter distributions is taken as the systematic uncertainty.

A summary of the systematic uncertainties is given in Table 4. After adding the systematic uncertainties in quadrature, we measure the following values of the CP -violating phase and

the width difference between the two B_s^0 mass eigenstates:

$$\begin{aligned}\phi_s &= -11 \pm 50 \text{ (stat)} \pm 10 \text{ (syst) mrad}, \\ \Delta\Gamma_s &= 0.114 \pm 0.014 \text{ (stat)} \pm 0.007 \text{ (syst) ps}^{-1}.\end{aligned}$$

The $|\lambda|$ parameter is measured to be $|\lambda| = 0.972 \pm 0.026 \text{ (stat)} \pm 0.008 \text{ (syst)}$, consistent with no direct CP violation ($|\lambda| = 1$). The average of the heavy and light B_s^0 mass eigenstate decay widths is determined to be $\Gamma_s = 0.6531 \pm 0.0042 \text{ (stat)} \pm 0.0026 \text{ (syst) ps}^{-1}$, consistent with the world-average value $\Gamma_s = 0.6624 \pm 0.0018 \text{ ps}^{-1}$ [31]. The mass difference between the heavy and light B_s^0 meson mass eigenstates is measured to be $\Delta m_s = 17.51^{+0.10}_{-0.09} \text{ (stat)} \pm 0.03 \text{ (syst) } \hbar \text{ ps}^{-1}$, consistent with the theoretical prediction $\Delta m_s = 18.77 \pm 0.86 \hbar \text{ ps}^{-1}$ [4], and in slight tension with the world-average value $\Delta m_s = 17.757 \pm 0.021 \hbar \text{ ps}^{-1}$ [31]. The uncertainties in all these measured parameters are dominated by the statistical component. This analysis represents the first measurement by CMS of the mass difference Δm_s between the heavy and light B_s^0 mass eigenstates and of the direct CP observable $|\lambda|$.

7 Combination with 8 TeV results

The results presented in this Letter are in agreement with the earlier CMS result at a center-of-mass energy of 8 TeV [14]. As explained in Section 1, both measurements are performed with a similar number of events, with the one at $\sqrt{s} = 13 \text{ TeV}$ having a higher tagging efficiency. This leads to an improvement in the uncertainty in quantities that require tagging, such as ϕ_s , while but the uncertainties in those that do not use tagging, such as $\Delta\Gamma_s$, depend on the raw number of events and are not improved relative to the 8 TeV result. The two sets of results are combined using the BLUE method [48, 49] as implemented in the ROOT package [50–52] using the following physics parameters: ϕ_s , $\Delta\Gamma_s$, Γ_s , $|A_0|^2$, $|A_\perp|^2$, $|A_S|^2$, δ_\parallel , δ_\perp , and $\delta_{S\perp}$. The statistical correlations between the parameters obtained in each measurement are taken into account as well as the correlations of the systematic uncertainties discussed in Section 6. Different sources of systematic uncertainties are assumed to be uncorrelated. The systematic uncertainty correlation between the parameters of the 8 TeV result is assumed to be zero. This assumption has been found to not impact the results in a noticeable way. Since the muon tagging, the efficiency evaluation, and part of the fit model are different in the two measurements, the respective systematic uncertainties are treated as uncorrelated between the two sets of results. The combined results for the CP -violating phase and lifetime difference between the two mass eigenstates are:

$$\begin{aligned}\phi_s &= -21 \pm 44 \text{ (stat)} \pm 10 \text{ (syst) mrad}, \\ \Delta\Gamma_s &= 0.1032 \pm 0.0095 \text{ (stat)} \pm 0.0048 \text{ (syst) ps}^{-1},\end{aligned}$$

with a correlation between the two parameters of $+0.02$. The full combination results and the correlations between the various extracted parameters are reported in Appendix A.

The two-dimensional ϕ_s vs. $\Delta\Gamma_s$ likelihood contours at 68% confidence level (CL) for the individual and combined results, as well as the SM prediction, are shown in Fig. 6. The contours for the individual results are obtained with likelihood scans, which are used to obtain the combined contour. The contours only account for the statistical uncertainty and the correlation between the two scanned variables, while the results from the combination obtained using the BLUE method take into account the statistical and systematic correlations of a wider range of variables. The results are in agreement with each other and with the SM predictions.

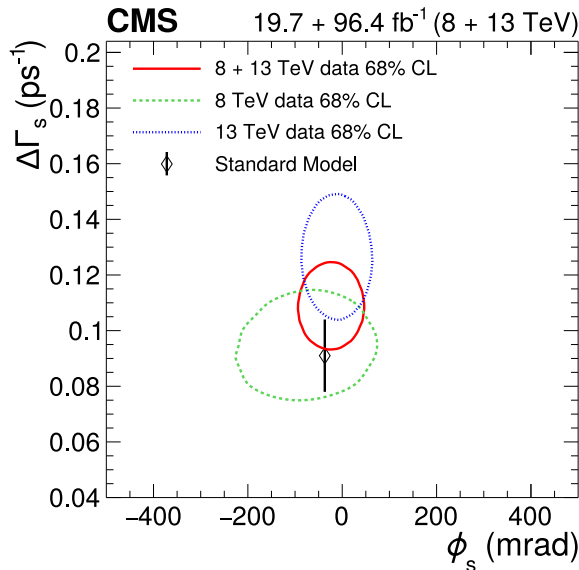


Figure 6: The two-dimensional likelihood contours at 68% CL in the ϕ_s - $\Delta\Gamma_s$ plane, for the CMS 8 TeV (dashed line), 13 TeV (dotted line), and combined (solid line) results. The contours for the individual results are obtained with likelihood scans, which are used to obtain the combined contour. In all contours only statistical uncertainties are taken into account. The SM prediction is shown with the diamond marker [1, 4].

8 Summary

The CP -violating phase ϕ_s and the decay width difference $\Delta\Gamma_s$ between the light and heavy B_s^0 meson mass eigenstates are measured using a total of 48 500 $B_s^0 \rightarrow J/\psi \phi(1020) \rightarrow \mu^+ \mu^- K^+ K^-$ signal events, collected by the CMS experiment at the LHC in proton-proton collisions at $\sqrt{s} = 13$ TeV, corresponding to an integrated luminosity of 96.4 fb^{-1} . Events are selected using a trigger that requires an additional muon, which can be exploited to infer the flavor of the B_s^0 meson at the time of production. A novel opposite-side muon tagger based on deep neural networks has been developed to maximize the sensitivity of the present analysis. A high tagging power of $\approx 10\%$ is achieved, aided by the requirement of an additional muon in the signal sample imposed at the trigger level.

The CP -violating phase is measured to be $\phi_s = -11 \pm 50$ (stat) ± 10 (syst) mrad, consistent both with the SM prediction $\phi_s = -36.96^{+0.72}_{-0.84}$ mrad [1] and with the absence of CP violation in the mixing-decay interference. The decay width difference between the B_s^0 mass eigenstates is measured to be $\Delta\Gamma_s = 0.114 \pm 0.014$ (stat) ± 0.007 (syst) ps^{-1} , consistent with the theoretical prediction $\Delta\Gamma_s = 0.091 \pm 0.013 \text{ ps}^{-1}$ [4]. In addition, the CP -violating parameter $|\lambda|$ and the average lifetime of the heavy and light B_s^0 mass eigenstates, as well as their mass difference, have been measured. The uncertainties in all these measurements are dominated by the statistical components.

The results presented in this Letter are further combined with those obtained by CMS at $\sqrt{s} = 8$ TeV [14], yielding $\phi_s = -21 \pm 44$ (stat) ± 10 (syst) mrad and $\Delta\Gamma_s = 0.1032 \pm 0.0095$ (stat) ± 0.0048 (syst) ps^{-1} . These results are significantly more precise than those from the previous CMS measurement at 8 TeV, and can be used to further constrain possible new-physics effects in B_s^0 meson decay and mixing.

Acknowledgments

We congratulate our colleagues in the CERN accelerator departments for the excellent performance of the LHC and thank the technical and administrative staffs at CERN and at other CMS institutes for their contributions to the success of the CMS effort. In addition, we gratefully acknowledge the computing centers and personnel of the Worldwide LHC Computing Grid for delivering so effectively the computing infrastructure essential to our analyses. Finally, we acknowledge the enduring support for the construction and operation of the LHC and the CMS detector provided by the following funding agencies: BMBWF and FWF (Austria); FNRS and FWO (Belgium); CNPq, CAPES, FAPERJ, FAPERGS, and FAPESP (Brazil); MES (Bulgaria); CERN; CAS, MoST, and NSFC (China); COLCIENCIAS (Colombia); MSES and CSF (Croatia); RIF (Cyprus); SENESCYT (Ecuador); MoER, ERC IUT, PUT and ERDF (Estonia); Academy of Finland, MEC, and HIP (Finland); CEA and CNRS/IN2P3 (France); BMBF, DFG, and HGF (Germany); GSRT (Greece); NKFI (Hungary); DAE and DST (India); IPM (Iran); SFI (Ireland); INFN (Italy); MSIP and NRF (Republic of Korea); MES (Latvia); LAS (Lithuania); MOE and UM (Malaysia); BUAP, CINVESTAV, CONACYT, LNS, SEP, and UASLP-FAI (Mexico); MOS (Montenegro); MBIE (New Zealand); PAEC (Pakistan); MSHE and NSC (Poland); FCT (Portugal); JINR (Dubna); MON, RosAtom, RAS, RFBR, and NRC KI (Russia); MESTD (Serbia); SEIDI, CPAN, PCTI, and FEDER (Spain); MOSTR (Sri Lanka); Swiss Funding Agencies (Switzerland); MST (Taipei); ThEPCenter, IPST, STAR, and NSTDA (Thailand); TUBITAK and TAEK (Turkey); NASU (Ukraine); STFC (United Kingdom); DOE and NSF (USA).

Individuals have received support from the Marie-Curie program and the European Research Council and Horizon 2020 Grant, contract Nos. 675440, 752730, and 765710 (European Union); the Leventis Foundation; the A.P. Sloan Foundation; the Alexander von Humboldt Foundation; the Belgian Federal Science Policy Office; the Fonds pour la Formation à la Recherche dans l'Industrie et dans l'Agriculture (FRIA-Belgium); the Agentschap voor Innovatie door Wetenschap en Technologie (IWT-Belgium); the F.R.S.-FNRS and FWO (Belgium) under the "Excellence of Science – EOS" – be.h project n. 30820817; the Beijing Municipal Science & Technology Commission, No. Z191100007219010; the Ministry of Education, Youth and Sports (MEYS) of the Czech Republic; the Deutsche Forschungsgemeinschaft (DFG) under Germany's Excellence Strategy – EXC 2121 "Quantum Universe" – 390833306; the Lendület ("Momentum") Program and the János Bolyai Research Scholarship of the Hungarian Academy of Sciences, the New National Excellence Program ÚNKP, the NKFI research grants 123842, 123959, 124845, 124850, 125105, 128713, 128786, and 129058 (Hungary); the Council of Science and Industrial Research, India; the HOMING PLUS program of the Foundation for Polish Science, cofinanced from European Union, Regional Development Fund, the Mobility Plus program of the Ministry of Science and Higher Education, the National Science Center (Poland), contracts Harmonia 2014/14/M/ST2/00428, Opus 2014/13/B/ST2/02543, 2014/15/B/ST2/03998, and 2015/19/B/ST2/02861, Sonata-bis 2012/07/E/ST2/01406; the National Priorities Research Program by Qatar National Research Fund; the Ministry of Science and Higher Education, project no. 02.a03.21.0005 (Russia); the Programa Estatal de Fomento de la Investigación Científica y Técnica de Excelencia María de Maeztu, grant MDM-2015-0509 and the Programa Severo Ochoa del Principado de Asturias; the Thalís and Aristeia programs cofinanced by EU-ESF and the Greek NSRF; the Rachadapisek Sompot Fund for Postdoctoral Fellowship, Chulalongkorn University and the Chulalongkorn Academic into Its 2nd Century Project Advancement Project (Thailand); the Kavli Foundation; the Nvidia Corporation; the SuperMicro Corporation; the Welch Foundation, contract C-1845; and the Weston Havens Foundation (USA).

References

- [1] The CKMfitter Group Collaboration, “Predictions of selected flavour observables within the Standard Model”, *Phys. Rev. D* **84** (2011) 033005, doi:10.1103/PhysRevD.84.033005, arXiv:1106.4041. Updated with Summer 2019 results: http://ckmfitter.in2p3.fr/www/results/plots_summer19/num/ckmEval_results_summer19.pdf.
- [2] C.-W. Chiang et al., “New physics in $B_s^0 \rightarrow J/\psi\phi$: a general analysis”, *JHEP* **04** (2010) 031, doi:10.1007/JHEP04(2010)031, arXiv:0910.2929.
- [3] M. Artuso, G. Borissov, and A. Lenz, “CP violation in the B_s^0 system”, *Rev. Mod. Phys.* **88** (2016), no. 4, 045002, doi:10.1103/RevModPhys.88.045002, arXiv:1511.09466. [Addendum: *Rev.Mod.Phys.* 91, 049901 (2019)].
- [4] A. Lenz and G. Tetlalmatzi-Xolocotzi, “Model-independent bounds on new physics effects in non-leptonic tree-level decays of B-mesons”, *JHEP* **07** (2020) 177, doi:10.1007/JHEP07(2020)177, arXiv:1912.07621.
- [5] D0 Collaboration, “Measurement of B_s^0 mixing parameters from the flavor-tagged decay $B_s^0 \rightarrow J/\psi\phi$ ”, *Phys. Rev. Lett.* **101** (2008) 241801, doi:10.1103/PhysRevLett.101.241801, arXiv:0802.2255.
- [6] D0 Collaboration, “Measurement of the CP-violating phase $\phi_s^{J/\psi\phi}$ using the flavor-tagged decay $B_s^0 \rightarrow J/\psi\phi$ in 8 fb^{-1} of $p\bar{p}$ collisions”, *Phys. Rev. D* **85** (2012) 032006, doi:10.1103/PhysRevD.85.032006, arXiv:1109.3166.
- [7] CDF Collaboration, “First flavor-tagged determination of bounds on mixing-induced CP violation in $B_s^0 \rightarrow J/\psi\phi$ decays”, *Phys. Rev. Lett.* **100** (2008) 161802, doi:10.1103/PhysRevLett.100.161802, arXiv:0712.2397.
- [8] CDF Collaboration, “Measurement of the CP-violating phase $\beta_s^{J/\psi\phi}$ in $B_s^0 \rightarrow J/\psi\phi$ decays with the CDF II detector”, *Phys. Rev. D* **85** (2012) 072002, doi:10.1103/PhysRevD.85.072002, arXiv:1112.1726.
- [9] CDF Collaboration, “Measurement of the bottom-strange meson mixing phase in the full CDF data set”, *Phys. Rev. Lett.* **109** (2012) 171802, doi:10.1103/PhysRevLett.109.171802, arXiv:1208.2967.
- [10] ATLAS Collaboration, “Time-dependent angular analysis of the decay $B_s^0 \rightarrow J/\psi\phi$ and extraction of $\Delta\Gamma_s$ and the CP-violating weak phase ϕ_s by ATLAS”, *JHEP* **12** (2012) 072, doi:10.1007/JHEP12(2012)072, arXiv:1208.0572.
- [11] ATLAS Collaboration, “Flavor tagged time-dependent angular analysis of the $B_s^0 \rightarrow J/\psi\phi$ decay and extraction of $\Delta\Gamma_s$ and the weak phase ϕ_s in ATLAS”, *Phys. Rev. D* **90** (2014) 052007, doi:10.1103/PhysRevD.90.052007, arXiv:1407.1796.
- [12] ATLAS Collaboration, “Measurement of the CP-violating phase ϕ_s and the B_s meson decay width difference with $B_s^0 \rightarrow J/\psi\phi$ decays in ATLAS”, *JHEP* **12** (2016) 072, doi:10.1007/JHEP08(2016)147, arXiv:1601.03297.
- [13] ATLAS Collaboration, “Measurement of the CP-violating phase ϕ_s in $B_s^0 \rightarrow J/\psi\phi$ decays in ATLAS at 13 TeV”, (2020). arXiv:2001.07115. Submitted to EPJC.

-
- [14] CMS Collaboration, “Measurement of the CP-violating weak phase ϕ_s and the decay width difference $\Delta\Gamma_s$ using the $B_s^0 \rightarrow J/\psi \phi$ decay channel in pp collisions at $\sqrt{s} = 8$ TeV”, *Phys. Lett. B* **757** (2016) 97, doi:10.1016/j.physletb.2016.03.046, arXiv:1507.07527.
- [15] LHCb Collaboration, “Measurement of the CP-violating phase ϕ_s in $\bar{B}_s^0 \rightarrow J/\psi \pi^+ \pi^-$ decays”, *Phys. Lett. B* **713** (2012) 378, doi:10.1016/j.physletb.2012.06.032, arXiv:1204.5675.
- [16] LHCb Collaboration, “Measurement of CP violation and the B_s^0 meson decay width difference with $B_s^0 \rightarrow J/\psi K^+ K^-$ and $B_s^0 \rightarrow J/\psi \pi^+ \pi^-$ decays”, *Phys. Rev. D* **87** (2013) 112010, doi:10.1103/PhysRevD.87.112010, arXiv:1304.2600.
- [17] LHCb Collaboration, “Measurement of the CP-violating phase ϕ_s in $\bar{B}_s^0 \rightarrow J/\psi \pi^+ \pi^-$ decays”, *Phys. Lett. B* **736** (2014) 186, doi:10.1016/j.physletb.2014.06.079, arXiv:1405.4140.
- [18] LHCb Collaboration, “Precision measurement of CP violation in $B_s^0 \rightarrow J/\psi K^+ K^-$ decays”, *Phys. Rev. Lett.* **114** (2015) 041801, doi:10.1103/PhysRevLett.114.041801, arXiv:1411.3104.
- [19] LHCb Collaboration, “Updated measurement of time-dependent CP-violating observables in $B_s^0 \rightarrow J/\psi K^+ K^-$ decays”, *Eur. Phys. J. C* **79** (2019), no. 8, 706, doi:10.1140/epjc/s10052-019-7159-8, arXiv:1906.08356. [Erratum: doi:10.1140/epjc/s10052-020-7875-0].
- [20] LHCb Collaboration, “First study of the CP-violating phase and decay-width difference in $B_s^0 \rightarrow \psi(2S) \phi$ ”, *Phys. Lett. B* **762** (2016) 253, doi:10.1016/j.physletb.2016.09.028, arXiv:1608.04855.
- [21] LHCb Collaboration, “Measurement of the CP-violating phase ϕ_s in $\bar{B}_s^0 \rightarrow D_s^+ D_s^-$ decays”, *Phys. Rev. Lett.* **113** (2014) 211801, doi:10.1103/PhysRevLett.113.211801, arXiv:1409.4619.
- [22] A. S. Dighe, I. Dunietz, and R. Fleischer, “Extracting CKM phases and B_s^0 - \bar{B}_s^0 mixing parameters from angular distributions of non-leptonic B decays”, *Eur. Phys. J. C* **6** (1999) 647, doi:10.1007/s100529800954, arXiv:hep-ph/9804253.
- [23] A. S. Dighe, I. Dunietz, H. J. Lipkin, and J. L. Rosner, “Angular distributions and lifetime differences in $B_s^0 \rightarrow J/\psi \phi$ decays”, *Phys. Lett. B* **369** (1996) 144, doi:10.1016/0370-2693(95)01523-X, arXiv:hep-ph/9511363.
- [24] G. C. Branco, L. Lavoura, and J. P. Silva, “CP Violation”, volume 103 of *International Series of Monographs on Physics*. Clarendon Press, Oxford, UK, 1999. ISBN 0198503997.
- [25] CMS Collaboration, “Performance of the CMS muon detector and muon reconstruction with proton-proton collisions at $\sqrt{s} = 13$ TeV”, *JINST* **13** (2018) P06015, doi:10.1088/1748-0221/13/06/P06015, arXiv:1804.04528.
- [26] CMS Collaboration, “The CMS trigger system”, *JINST* **12** (2017) P01020, doi:10.1088/1748-0221/12/01/P01020, arXiv:1609.02366.
- [27] CMS Collaboration, “The CMS Experiment at the CERN LHC”, *JINST* **3** (2008) S08004, doi:10.1088/1748-0221/3/08/S08004.

- [28] I. Antcheva et al., “ROOT — A C++ framework for petabyte data storage, statistical analysis and visualization”, *Comput. Phys. Commun.* **180** (2009) 2499, doi:10.1016/j.cpc.2009.08.005, arXiv:1508.07749.
- [29] H. Voss, A. Höcker, J. Stelzer, and F. Tegenfeldt, “TMVA, the toolkit for multivariate data analysis with ROOT”, in *XIth International Workshop on Advanced Computing and Analysis Techniques in Physics Research (ACAT)*, p. 40. 2007. arXiv:physics/0703039. [PoS(ACAT)040]. doi:10.22323/1.050.0040.
- [30] R. Frühwirth, “Application of Kalman filtering to track and vertex fitting”, *Nucl. Instrum. Meth. A* **262** (1987) 444, doi:10.1016/0168-9002(87)90887-4.
- [31] Particle Data Group, M. Tanabashi et al., “Review of particle physics”, *Phys. Rev. D* **98** (2018) 030001, doi:10.1103/PhysRevD.98.030001.
- [32] CMS Collaboration, “Description and performance of track and primary-vertex reconstruction with the CMS tracker”, *JINST* **9** (2014) P10009, doi:10.1088/1748-0221/9/10/P10009, arXiv:1405.6569.
- [33] T. Sjöstrand et al., “An introduction to PYTHIA 8.2”, *Comput. Phys. Commun.* **191** (2015) 159, doi:10.1016/j.cpc.2015.01.024, arXiv:1410.3012.
- [34] CMS Collaboration, “Extraction and validation of a new set of CMS PYTHIA8 tunes from underlying-event measurements”, *Eur. Phys. J. C* **80** (2020) 4, doi:10.1140/epjc/s10052-019-7499-4, arXiv:1903.12179.
- [35] NNPDF Collaboration, “Parton distributions from high-precision collider data”, *Eur. Phys. J. C* **77** (2017) 663, doi:10.1140/epjc/s10052-017-5199-5, arXiv:1706.00428.
- [36] D. J. Lange, “The EvtGen particle decay simulation package”, *Nucl. Instrum. Meth. A* **462** (2001) 152, doi:10.1016/S0168-9002(01)00089-4.
- [37] E. Barberio, B. van Eijk, and Z. Waş, “PHOTOS — a universal Monte Carlo for QED radiative corrections in decays”, *Comput. Phys. Commun.* **66** (1991) 115, doi:10.1016/0010-4655(91)90012-A.
- [38] E. Barberio and Z. Waş, “PHOTOS — a universal Monte Carlo for QED radiative corrections: version 2.0”, *Comput. Phys. Commun.* **79** (1994) 291, doi:10.1016/0010-4655(94)90074-4.
- [39] GEANT4 Collaboration, “GEANT4 — a simulation toolkit”, *Nucl. Instrum. Meth. A* **506** (2003) 250, doi:10.1016/S0168-9002(03)01368-8.
- [40] F. Chollet et al., “Keras”. <https://keras.io>, 2015.
- [41] CMS Collaboration, “Particle-flow reconstruction and global event description with the CMS detector”, *JINST* **12** (2017) P10003, doi:10.1088/1748-0221/12/10/P10003, arXiv:1706.04965.
- [42] D. Kingma and J. Ba, “Adam: A method for stochastic optimization”, (12, 2014). arXiv:1412.6980.
- [43] W. Verkerke and D. Kirkby, “The roofit toolkit for data modeling”, 2003.

- [44] LHCb Collaboration, "Determination of the sign of the decay width difference in the B_s system", *Phys. Rev. Lett.* **108** (2012) 241801, doi:10.1103/PhysRevLett.108.241801, arXiv:1202.4717.
- [45] N. L. Johnson, "Systems of frequency curves generated by methods of translation", *Biometrika* **36** (1949) 149, doi:10.1093/biomet/36.1-2.149.
- [46] M. Rosenblatt, "Remarks on some nonparametric estimates of a density function", *Ann. Math. Statist.* **27** (1956) 832, doi:10.1214/aoms/1177728190.
- [47] E. Parzen, "On estimation of a probability density function and mode", *Ann. Math. Statist.* **33** (1962) 1065, doi:10.1214/aoms/1177704472.
- [48] L. Lyons, D. Gibaut, and P. Clifford, "How to combine correlated estimates of a single physical quantity", *Nucl. Instrum. Meth. A* **270** (1988) 110, doi:10.1016/0168-9002(88)90018-6.
- [49] A. Valassi, "Combining correlated measurements of several different physical quantities", *Nucl. Instrum. Meth. A* **500** (2003) 391, doi:10.1016/S0168-9002(03)00329-2.
- [50] R. Brun and F. Rademakers, "ROOT: An object oriented data analysis framework", *Nucl. Instrum. Meth. A* **389** (1997) 81, doi:10.1016/S0168-9002(97)00048-X.
- [51] R. Nisius, "On the combination of correlated estimates of a physics observable", *Eur. Phys. J. C* **74** (2014), no. 8, 3004, doi:10.1140/epjc/s10052-014-3004-2, arXiv:1402.4016.
- [52] R. Nisius, "BLUE: combining correlated estimates of physics observables within ROOT using the Best Linear Unbiased Estimate method", *SoftwareX* **11** (1, 2020) 100468, doi:10.1016/j.softx.2020.100468, arXiv:2001.10310.

B The CMS Collaboration

Yerevan Physics Institute, Yerevan, Armenia

A.M. Sirunyan[†], A. Tumasyan

Institut für Hochenergiephysik, Wien, Austria

W. Adam, F. Ambrogio, T. Bergauer, M. Dragicevic, J. Erö, A. Escalante Del Valle, R. Frühwirth¹, M. Jeitler¹, N. Krammer, L. Lechner, D. Liko, T. Madlener, I. Mikulec, F.M. Pitters, N. Rad, J. Schieck¹, R. Schöfbeck, M. Spanring, S. Templ, W. Waltenberger, C.-E. Wulz¹, M. Zarucki

Institute for Nuclear Problems, Minsk, Belarus

V. Chekhovskiy, A. Litomin, V. Makarenko, J. Suarez Gonzalez

Universiteit Antwerpen, Antwerpen, Belgium

M.R. Darwish², E.A. De Wolf, D. Di Croce, X. Janssen, T. Kello³, A. Lelek, M. Pieters, H. Rejeb Sfar, H. Van Haevermaet, P. Van Mechelen, S. Van Putte, N. Van Remortel

Vrije Universiteit Brussel, Brussel, Belgium

F. Blekman, E.S. Bols, S.S. Chhibra, J. D'Hondt, J. De Clercq, D. Lontkovskiy, S. Lowette, I. Marchesini, S. Moortgat, A. Morton, Q. Python, S. Tavernier, W. Van Doninck, P. Van Mulders

Université Libre de Bruxelles, Bruxelles, Belgium

D. Beghin, B. Bilin, B. Clerboux, G. De Lentdecker, H. Delannoy, B. Dorney, L. Favart, A. Grebenyuk, A.K. Kalsi, I. Makarenko, L. Moureaux, L. Pétrelle, A. Popov, N. Postiau, E. Starling, L. Thomas, C. Vander Velde, P. Vanlaer, D. Vannerom, L. Wezenbeek

Ghent University, Ghent, Belgium

T. Cornelis, D. Dobur, M. Gruchala, I. Khvastunov⁴, M. Niedziela, C. Roskas, K. Skovpen, M. Tytgat, W. Verbeke, B. Vermassen, M. Vit

Université Catholique de Louvain, Louvain-la-Neuve, Belgium

G. Bruno, F. Bury, C. Caputo, P. David, C. Delaere, M. Delcourt, I.S. Donertas, A. Giammanco, V. Lemaitre, K. Mondal, J. Prisciandaro, A. Taliencio, M. Teklishyn, P. Vischia, S. Wuyckens, J. Zobec

Centro Brasileiro de Pesquisas Físicas, Rio de Janeiro, Brazil

G.A. Alves, G. Correia Silva, C. Hensel, A. Moraes

Universidade do Estado do Rio de Janeiro, Rio de Janeiro, Brazil

W.L. Aldá Júnior, E. Belchior Batista Das Chagas, H. BRANDAO MALBOUISSON, W. Carvalho, J. Chinellato⁵, E. Coelho, E.M. Da Costa, G.G. Da Silveira⁶, D. De Jesus Damiao, S. Fonseca De Souza, J. Martins⁷, D. Matos Figueiredo, M. Medina Jaime⁸, M. Melo De Almeida, C. Mora Herrera, L. Mundim, H. Nogima, P. Rebello Teles, L.J. Sanchez Rosas, A. Santoro, S.M. Silva Do Amaral, A. Sznajder, M. Thiel, E.J. Tonelli Manganote⁵, F. Torres Da Silva De Araujo, A. Vilela Pereira

Universidade Estadual Paulista ^a, Universidade Federal do ABC ^b, São Paulo, Brazil

C.A. Bernardes^a, L. Calligaris^a, T.R. Fernandez Perez Tomei^a, E.M. Gregores^b, D.S. Lemos^a, P.G. Mercadante^b, S.F. Novaes^a, Sandra S. Padula^a

Institute for Nuclear Research and Nuclear Energy, Bulgarian Academy of Sciences, Sofia, Bulgaria

A. Aleksandrov, G. Antchev, I. Atanasov, R. Hadjiiska, P. Iaydjiev, M. Misheva, M. Rodozov, M. Shopova, G. Sultanov

University of Sofia, Sofia, Bulgaria

M. Bonchev, A. Dimitrov, T. Ivanov, L. Litov, B. Pavlov, P. Petkov, A. Petrov

Beihang University, Beijing, China

W. Fang³, Q. Guo, H. Wang, L. Yuan

Department of Physics, Tsinghua University, Beijing, China

M. Ahmad, Z. Hu, Y. Wang

Institute of High Energy Physics, Beijing, China

E. Chapon, G.M. Chen⁹, H.S. Chen⁹, M. Chen, D. Leggat, H. Liao, Z. Liu, R. Sharma, A. Spiezia, J. Tao, J. Thomas-wilsker, J. Wang, H. Zhang, S. Zhang⁹, J. Zhao

State Key Laboratory of Nuclear Physics and Technology, Peking University, Beijing, China

A. Agapitos, Y. Ban, C. Chen, A. Levin, J. Li, Q. Li, M. Lu, X. Lyu, Y. Mao, S.J. Qian, D. Wang, Q. Wang, J. Xiao

Sun Yat-Sen University, Guangzhou, China

Z. You

Institute of Modern Physics and Key Laboratory of Nuclear Physics and Ion-beam Application (MOE) - Fudan University, Shanghai, China

X. Gao³

Zhejiang University, Hangzhou, China

M. Xiao

Universidad de Los Andes, Bogota, Colombia

C. Avila, A. Cabrera, C. Florez, J. Fraga, A. Sarkar, M.A. Segura Delgado

Universidad de Antioquia, Medellin, Colombia

J. Jaramillo, J. Mejia Guisao, F. Ramirez, J.D. Ruiz Alvarez, C.A. Salazar González, N. Vanegas Arbelaez

University of Split, Faculty of Electrical Engineering, Mechanical Engineering and Naval Architecture, Split, Croatia

D. Giljanovic, N. Godinovic, D. Lelas, I. Puljak, T. Sculac

University of Split, Faculty of Science, Split, Croatia

Z. Antunovic, M. Kovac

Institute Rudjer Boskovic, Zagreb, Croatia

V. Brigljevic, D. Ferencek, D. Majumder, B. Mesic, M. Roguljic, A. Starodumov¹⁰, T. Susa

University of Cyprus, Nicosia, Cyprus

M.W. Ather, A. Attikis, E. Erodotou, A. Ioannou, G. Kole, M. Kolosova, S. Konstantinou, G. Mavromanolakis, J. Mousa, C. Nicolaou, F. Ptochos, P.A. Razis, H. Rykaczewski, H. Saka, D. Tsiakkouri

Charles University, Prague, Czech Republic

M. Finger¹¹, M. Finger Jr.¹¹, A. Kveton, J. Tomsa

Escuela Politecnica Nacional, Quito, Ecuador

E. Ayala

Universidad San Francisco de Quito, Quito, Ecuador

E. Carrera Jarrin

Academy of Scientific Research and Technology of the Arab Republic of Egypt, Egyptian Network of High Energy Physics, Cairo, Egypt

A.A. Abdelalim^{12,13}, S. Abu Zeid¹⁴, S. Khalil¹³

Center for High Energy Physics (CHEP-FU), Fayoum University, El-Fayoum, Egypt

A. Lotfy, M.A. Mahmoud

National Institute of Chemical Physics and Biophysics, Tallinn, Estonia

S. Bhowmik, A. Carvalho Antunes De Oliveira, R.K. Dewanjee, K. Ehataht, M. Kadastik, M. Raidal, C. Veelken

Department of Physics, University of Helsinki, Helsinki, Finland

P. Eerola, L. Forthomme, H. Kirschenmann, K. Osterberg, M. Voutilainen

Helsinki Institute of Physics, Helsinki, Finland

E. Brücken, F. Garcia, J. Havukainen, V. Karimäki, M.S. Kim, R. Kinnunen, T. Lampén, K. Lassila-Perini, S. Laurila, S. Lehti, T. Lindén, H. Siikonen, E. Tuominen, J. Tuominiemi

Lappeenranta University of Technology, Lappeenranta, Finland

P. Luukka, T. Tuuva

IRFU, CEA, Université Paris-Saclay, Gif-sur-Yvette, France

M. Besancon, F. Couderc, M. Dejardin, D. Denegri, J.L. Faure, F. Ferri, S. Ganjour, A. Givernaud, P. Gras, G. Hamel de Monchenault, P. Jarry, B. Lenzi, E. Locci, J. Malcles, J. Rander, A. Rosowsky, M.Ö. Sahin, A. Savoy-Navarro¹⁵, M. Titov, G.B. Yu

Laboratoire Leprince-Ringuet, CNRS/IN2P3, Ecole Polytechnique, Institut Polytechnique de Paris, Paris, France

S. Ahuja, C. Amendola, F. Beaudette, M. Bonanomi, P. Busson, C. Charlot, O. Davignon, B. Diab, G. Falmagne, R. Granier de Cassagnac, I. Kucher, A. Lobanov, C. Martin Perez, M. Nguyen, C. Ochando, P. Paganini, J. Rembser, R. Salerno, J.B. Sauvan, Y. Sirois, A. Zabi, A. Zghiche

Université de Strasbourg, CNRS, IPHC UMR 7178, Strasbourg, France

J.-L. Agram¹⁶, J. Andrea, D. Bloch, G. Bourgatte, J.-M. Brom, E.C. Chabert, C. Collard, J.-C. Fontaine¹⁶, D. Gelé, U. Goerlach, C. Grimault, A.-C. Le Bihan, P. Van Hove

Université de Lyon, Université Claude Bernard Lyon 1, CNRS-IN2P3, Institut de Physique Nucléaire de Lyon, Villeurbanne, France

E. Asilar, S. Beauceron, C. Bernet, G. Boudoul, C. Camen, A. Carle, N. Chanon, D. Contardo, P. Depasse, H. El Mamouni, J. Fay, S. Gascon, M. Gouzevitch, B. Ille, Sa. Jain, I.B. Laktineh, H. Lattaud, A. Lesauvage, M. Lethuillier, L. Mirabito, L. Torterotot, G. Touquet, M. Vander Donckt, S. Viret

Georgian Technical University, Tbilisi, Georgia

T. Toriashvili¹⁷, Z. Tsamalaidze¹¹

RWTH Aachen University, I. Physikalisches Institut, Aachen, Germany

L. Feld, K. Klein, M. Lipinski, D. Meuser, A. Pauls, M. Preuten, M.P. Rauch, J. Schulz, M. Teroerde

RWTH Aachen University, III. Physikalisches Institut A, Aachen, Germany

D. Eliseev, M. Erdmann, P. Fackeldey, B. Fischer, S. Ghosh, T. Hebbeker, K. Hoepfner, H. Keller, L. Mastrolorenzo, M. Merschmeyer, A. Meyer, P. Millet, G. Mocellin, S. Mondal, S. Mukherjee, D. Noll, A. Novak, T. Pook, A. Pozdnyakov, T. Quast, M. Radziej, Y. Rath, H. Reithler, J. Roemer, A. Schmidt, S.C. Schuler, A. Sharma, S. Wiedenbeck, S. Zaleski

RWTH Aachen University, III. Physikalisches Institut B, Aachen, Germany

C. Dziwok, G. Flügge, W. Haj Ahmad¹⁸, O. Hlushchenko, T. Kress, A. Nowack, C. Pistone, O. Pooth, D. Roy, H. Sert, A. Stahl¹⁹, T. Ziemons

Deutsches Elektronen-Synchrotron, Hamburg, Germany

H. Aarup Petersen, M. Aldaya Martin, P. Asmuss, I. Babounikau, S. Baxter, O. Behnke, A. Bermúdez Martínez, A.A. Bin Anuar, K. Borras²⁰, V. Botta, D. Brunner, A. Campbell, A. Cardini, P. Connor, S. Consuegra Rodríguez, V. Danilov, A. De Wit, M.M. Defranchis, L. Didukh, D. Domínguez Damiani, G. Eckerlin, D. Eckstein, T. Eichhorn, A. Elwood, L.I. Estevez Banos, E. Gallo²¹, A. Geiser, A. Giraldi, A. Grohsjean, M. Guthoff, A. Harb, A. Jafari²², N.Z. Jomhari, H. Jung, A. Kasem²⁰, M. Kasemann, H. Kaveh, J. Keaveney, C. Kleinwort, J. Knolle, D. Krücker, W. Lange, T. Lenz, J. Lidrych, K. Lipka, W. Lohmann²³, R. Mankel, I.-A. Melzer-Pellmann, J. Metwally, A.B. Meyer, M. Meyer, M. Missiroli, J. Mnich, A. Mussgiller, V. Myronenko, Y. Otariid, D. Pérez Adán, S.K. Pflitsch, D. Pitzl, A. Raspereza, A. Saggio, A. Saibel, M. Savitskyi, V. Scheurer, P. Schütze, C. Schwanenberger, R. Shevchenko, A. Singh, R.E. Sosa Ricardo, H. Tholen, N. Tonon, O. Turkot, A. Vagnerini, M. Van De Klundert, R. Walsh, D. Walter, Y. Wen, K. Wichmann, C. Wissing, S. Wuchterl, O. Zenaiev, R. Zlebcik

University of Hamburg, Hamburg, Germany

R. Aggleton, S. Bein, L. Benato, A. Benecke, K. De Leo, T. Dreyer, A. Ebrahimi, F. Feindt, A. Fröhlich, C. Garbers, E. Garutti, D. Gonzalez, P. Gunnellini, J. Haller, A. Hinzmann, A. Karavdina, G. Kasieczka, R. Klanner, R. Kogler, S. Kurz, V. Kutzner, J. Lange, T. Lange, A. Malara, J. Multhaupt, C.E.N. Niemeyer, A. Nigamova, K.J. Pena Rodriguez, O. Rieger, P. Schleper, S. Schumann, J. Schwandt, D. Schwarz, J. Sonneveld, H. Stadie, G. Steinbrück, B. Vormwald, I. Zoi

Karlsruher Institut fuer Technologie, Karlsruhe, Germany

M. Baselga, S. Baur, J. Bechtel, T. Berger, E. Butz, R. Caspart, T. Chwalek, W. De Boer, A. Dierlamm, A. Droll, K. El Morabit, N. Faltermann, K. Flöh, M. Giffels, A. Gottmann, F. Hartmann¹⁹, C. Heidecker, U. Husemann, M.A. Iqbal, I. Katkov²⁴, P. Keicher, R. Koppenhöfer, S. Kudella, S. Maier, M. Metzler, S. Mitra, M.U. Mozer, D. Müller, Th. Müller, M. Musich, G. Quast, K. Rabbertz, J. Rauser, D. Savoieu, D. Schäfer, M. Schnepf, M. Schröder, D. Seith, I. Shvetsov, H.J. Simonis, R. Ulrich, M. Wassmer, M. Weber, C. Wöhrmann, R. Wolf, S. Wozniowski

Institute of Nuclear and Particle Physics (INPP), NCSR Demokritos, Aghia Paraskevi, Greece

G. Anagnostou, P. Asenov, G. Daskalakis, T. Geralis, A. Kyriakis, D. Loukas, G. Paspalaki, A. Stakia

National and Kapodistrian University of Athens, Athens, Greece

M. Diamantopoulou, D. Karasavvas, G. Karathanasis, P. Kontaxakis, C.K. Koraka, A. Manousakis-katsikakis, A. Panagiotou, I. Papavergou, N. Saoulidou, K. Theofilatos, K. Vellidis, E. Vourliotis

National Technical University of Athens, Athens, Greece

G. Bakas, K. Kousouris, I. Papakrivopoulos, G. Tsipolitis, A. Zacharopoulou

University of Ioánnina, Ioánnina, Greece

I. Evangelou, C. Foudas, P. Gianneios, P. Katsoulis, P. Kokkas, S. Mallios, K. Manitará, N. Manthos, I. Papadopoulos, J. Strogas

MTA-ELTE Lendület CMS Particle and Nuclear Physics Group, Eötvös Loránd University, Budapest, Hungary

M. Bartók²⁵, R. Chudasama, M. Csanad, M.M.A. Gadallah²⁶, S. Lökös²⁷, P. Major, K. Mandal, A. Mehta, G. Pasztor, O. Surányi, G.I. Veres

Wigner Research Centre for Physics, Budapest, Hungary

G. Bencze, C. Hajdu, D. Horvath²⁸, F. Sikler, V. Veszpremi, G. Vesztergombi[†]

Institute of Nuclear Research ATOMKI, Debrecen, Hungary

S. Czellar, J. Karancsi²⁵, J. Molnar, Z. Szillasi, D. Teyssier

Institute of Physics, University of Debrecen, Debrecen, Hungary

P. Raics, Z.L. Trocsanyi, B. Ujvari

Eszterhazy Karoly University, Karoly Robert Campus, Gyongyos, Hungary

T. Csorgo, F. Nemes, T. Novak

Indian Institute of Science (IISc), Bangalore, India

S. Choudhury, J.R. Komaragiri, D. Kumar, L. Panwar, P.C. Tiwari

National Institute of Science Education and Research, HBNI, Bhubaneswar, India

S. Bahinipati²⁹, D. Dash, C. Kar, P. Mal, T. Mishra, V.K. Muraleedharan Nair Bindhu, A. Nayak³⁰, D.K. Sahoo²⁹, N. Sur, S.K. Swain

Panjab University, Chandigarh, India

S. Bansal, S.B. Beri, V. Bhatnagar, S. Chauhan, N. Dhingra³¹, R. Gupta, A. Kaur, A. Kaur, S. Kaur, P. Kumari, M. Lohan, M. Meena, K. Sandeep, S. Sharma, J.B. Singh, A.K. Viridi

University of Delhi, Delhi, India

A. Ahmed, A. Bhardwaj, B.C. Choudhary, R.B. Garg, M. Gola, S. Keshri, A. Kumar, M. Naimuddin, P. Priyanka, K. Ranjan, A. Shah

Saha Institute of Nuclear Physics, HBNI, Kolkata, India

M. Bharti³², R. Bhattacharya, S. Bhattacharya, D. Bhowmik, S. Dutta, S. Ghosh, B. Gomber³³, M. Maity³⁴, S. Nandan, P. Palit, A. Purohit, P.K. Rout, G. Saha, S. Sarkar, M. Sharan, B. Singh³², S. Thakur³²

Indian Institute of Technology Madras, Madras, India

P.K. Behera, S.C. Behera, P. Kalbhor, A. Muhammad, R. Pradhan, P.R. Pujahari, A. Sharma, A.K. Sikdar

Bhabha Atomic Research Centre, Mumbai, India

D. Dutta, V. Jha, V. Kumar, D.K. Mishra, K. Naskar³⁵, P.K. Netrakanti, L.M. Pant, P. Shukla

Tata Institute of Fundamental Research-A, Mumbai, India

T. Aziz, M.A. Bhat, S. Dugad, R. Kumar Verma, U. Sarkar

Tata Institute of Fundamental Research-B, Mumbai, India

S. Banerjee, S. Bhattacharya, S. Chatterjee, P. Das, M. Guchait, S. Karmakar, S. Kumar, G. Majumder, K. Mazumdar, S. Mukherjee, D. Roy, N. Sahoo

Indian Institute of Science Education and Research (IISER), Pune, India

S. Dube, B. Kansal, A. Kapoor, K. Kothekar, S. Pandey, A. Rane, A. Rastogi, S. Sharma

Department of Physics, Isfahan University of Technology, Isfahan, Iran

H. Bakhshiansohi³⁶

Institute for Research in Fundamental Sciences (IPM), Tehran, Iran

S. Chenarani³⁷, S.M. Etesami, M. Khakzad, M. Mohammadi Najafabadi, M. Naseri

University College Dublin, Dublin, Ireland

M. Felcini, M. Grunewald

INFN Sezione di Bari ^a, Università di Bari ^b, Politecnico di Bari ^c, Bari, Italy

M. Abbrescia^{a,b}, R. Aly^{a,b,38}, C. Aruta^{a,b}, A. Colaleo^a, D. Creanza^{a,c}, N. De Filippis^{a,c}, M. De Palma^{a,b}, A. Di Florio^{a,b}, A. Di Pilato^{a,b}, W. Elmetenawee^{a,b}, L. Fiore^a, A. Gelmi^{a,b}, M. Gul^a, G. Iaselli^{a,c}, M. Ince^{a,b}, S. Lezki^{a,b}, G. Maggi^{a,c}, M. Maggi^a, I. Margjeka^{a,b}, J.A. Merlin^a, S. My^{a,b}, S. Nuzzo^{a,b}, A. Pompili^{a,b}, G. Pugliese^{a,c}, G. Selvaggi^{a,b}, L. Silvestris^a, F.M. Simone^{a,b}, R. Venditti^a, P. Verwilligen^a

INFN Sezione di Bologna ^a, Università di Bologna ^b, Bologna, Italy

G. Abbiendi^a, C. Battilana^{a,b}, D. Bonacorsi^{a,b}, L. Borgonovi^{a,b}, S. Braibant-Giacomelli^{a,b}, L. Brigliadori^{a,b}, R. Campanini^{a,b}, P. Capiluppi^{a,b}, A. Castro^{a,b}, F.R. Cavallo^a, C. Ciocca^a, M. Cuffiani^{a,b}, G.M. Dallavalle^a, T. Diotallevi^{a,b}, F. Fabbri^a, A. Fanfani^{a,b}, E. Fontanesi^{a,b}, P. Giacomelli^a, C. Grandi^a, L. Guiducci^{a,b}, F. Iemmi^{a,b}, S. Lo Meo^{a,39}, S. Marcellini^a, G. Masetti^a, F.L. Navarria^{a,b}, A. Perrotta^a, F. Primavera^{a,b}, T. Rovelli^{a,b}, G.P. Siroli^{a,b}, N. Tosi^a

INFN Sezione di Catania ^a, Università di Catania ^b, Catania, Italy

S. Albergo^{a,b,40}, S. Costa^{a,b}, A. Di Mattia^a, R. Potenza^{a,b}, A. Tricomi^{a,b,40}, C. Tuve^{a,b}

INFN Sezione di Firenze ^a, Università di Firenze ^b, Firenze, Italy

G. Barbagli^a, A. Cassese^a, R. Ceccarelli^{a,b}, V. Ciulli^{a,b}, C. Civinini^a, R. D'Alessandro^{a,b}, F. Fiori^a, E. Focardi^{a,b}, G. Latino^{a,b}, P. Lenzi^{a,b}, M. Lizzo^{a,b}, M. Meschini^a, S. Paoletti^a, R. Seidita^{a,b}, G. Sguazzoni^a, L. Viliani^a

INFN Laboratori Nazionali di Frascati, Frascati, Italy

L. Benussi, S. Bianco, D. Piccolo

INFN Sezione di Genova ^a, Università di Genova ^b, Genova, Italy

M. Bozzo^{a,b}, F. Ferro^a, R. Mulargia^{a,b}, E. Robutti^a, S. Tosi^{a,b}

INFN Sezione di Milano-Bicocca ^a, Università di Milano-Bicocca ^b, Milano, Italy

A. Benaglia^a, A. Beschi^{a,b}, F. Brivio^{a,b}, F. Cetorelli^{a,b}, V. Ciriolo^{a,b,19}, F. De Guio^{a,b}, M.E. Dinardo^{a,b}, P. Dini^a, S. Gennai^a, A. Ghezzi^{a,b}, P. Govoni^{a,b}, L. Guzzi^{a,b}, M. Malberti^a, S. Malvezzi^a, D. Menasce^a, F. Monti^{a,b}, L. Moroni^a, M. Paganoni^{a,b}, D. Pedrini^a, S. Ragazzi^{a,b}, T. Tabarelli de Fatis^{a,b}, D. Valsecchi^{a,b,19}, D. Zuolo^{a,b}

INFN Sezione di Napoli ^a, Università di Napoli 'Federico II' ^b, Napoli, Italy, Università della Basilicata ^c, Potenza, Italy, Università G. Marconi ^d, Roma, Italy

S. Buontempo^a, N. Cavallo^{a,c}, A. De Iorio^{a,b}, F. Fabozzi^{a,c}, F. Fienga^a, A.O.M. Iorio^{a,b}, L. Layer^{a,b}, L. Lista^{a,b}, S. Meola^{a,d,19}, P. Paolucci^{a,19}, B. Rossi^a, C. Sciacca^{a,b}, E. Voevodina^{a,b}

INFN Sezione di Padova ^a, Università di Padova ^b, Padova, Italy, Università di Trento ^c, Trento, Italy

P. Azzi^a, N. Bacchetta^a, D. Bisello^{a,b}, A. Boletti^{a,b}, A. Bragagnolo^{a,b}, R. Carlin^{a,b}, P. Checchia^a, P. De Castro Manzano^a, T. Dorigo^a, F. Gasparini^{a,b}, U. Gasparini^{a,b}, S.Y. Hoh^{a,b}, E. Lusiani, M. Margoni^{a,b}, A.T. Meneguzzo^{a,b}, M. Presilla^b, P. Ronchese^{a,b}, R. Rossin^{a,b}, F. Simonetto^{a,b}, G. Strong, A. Tiko^a, M. Tosi^{a,b}, H. YARAR^{a,b}, M. Zanetti^{a,b}, A. Zucchetta^{a,b}

INFN Sezione di Pavia ^a, Università di Pavia ^b, Pavia, Italy

A. Braghieri^a, S. Calzaferrri^{a,b}, D. Fiorina^{a,b}, P. Montagna^{a,b}, S.P. Ratti^{a,b}, V. Re^a, M. Ressegotti^{a,b}, C. Riccardi^{a,b}, P. Salvini^a, I. Vai^a, P. Vitulo^{a,b}

INFN Sezione di Perugia ^a, Università di Perugia ^b, Perugia, Italy

M. Biasini^{a,b}, G.M. Bilei^a, D. Ciangottini^{a,b}, L. Fanò^{a,b}, P. Lariccia^{a,b}, G. Mantovani^{a,b}, V. Mariani^{a,b}, M. Menichelli^a, F. Moscatelli^a, A. Rossi^{a,b}, A. Santocchia^{a,b}, D. Spiga^a, T. Tedeschi^{a,b}

INFN Sezione di Pisa ^a, Università di Pisa ^b, Scuola Normale Superiore di Pisa ^c, Pisa, Italy

K. Androsov^a, P. Azzurri^a, G. Bagliesi^a, V. Bertacchi^{a,c}, L. Bianchini^a, T. Boccali^a, R. Castaldi^a, M.A. Ciocci^{a,b}, R. Dell'Orso^a, M.R. Di Domenico^{a,b}, S. Donato^a, L. Giannini^{a,c}, A. Giassi^a, M.T. Grippo^a, F. Ligabue^{a,c}, E. Manca^{a,c}, G. Mandorli^{a,c}, A. Messineo^{a,b}, F. Palla^a, G. Ramirez-Sanchez^{a,c}, A. Rizzi^{a,b}, G. Rolandi^{a,c}, S. Roy Chowdhury^{a,c}, A. Scribano^a, N. Shafiei^{a,b}, P. Spagnolo^a, R. Tenchini^a, G. Tonelli^{a,b}, N. Turini^a, A. Venturi^a, P.G. Verdini^a

INFN Sezione di Roma ^a, Sapienza Università di Roma ^b, Rome, Italy

F. Cavallari^a, M. Cipriani^{a,b}, D. Del Re^{a,b}, E. Di Marco^a, M. Diemoz^a, E. Longo^{a,b}, P. Meridiani^a, G. Organtini^{a,b}, F. Pandolfi^a, R. Paramatti^{a,b}, C. Quaranta^{a,b}, S. Rahatlou^{a,b}, C. Rovelli^a, F. Santanastasio^{a,b}, L. Soffi^{a,b}, R. Tramontano^{a,b}

INFN Sezione di Torino ^a, Università di Torino ^b, Torino, Italy, Università del Piemonte Orientale ^c, Novara, Italy

N. Amapane^{a,b}, R. Arcidiacono^{a,c}, S. Argiro^{a,b}, M. Arneodo^{a,c}, N. Bartosik^a, R. Bellan^{a,b}, A. Bellora^{a,b}, C. Biino^a, A. Cappati^{a,b}, N. Cartiglia^a, S. Cometti^a, M. Costa^{a,b}, R. Covarelli^{a,b}, N. Demaria^a, B. Kiani^{a,b}, F. Legger^a, C. Mariotti^a, S. Maselli^a, E. Migliore^{a,b}, V. Monaco^{a,b}, E. Monteil^{a,b}, M. Monteno^a, M.M. Obertino^{a,b}, G. Ortona^a, L. Pacher^{a,b}, N. Pastrone^a, M. Pelliccioni^a, G.L. Pinna Angioni^{a,b}, M. Ruspa^{a,c}, R. Salvatico^{a,b}, F. Siviero^{a,b}, V. Sola^a, A. Solano^{a,b}, D. Soldi^{a,b}, A. Staiano^a, D. Trocino^{a,b}

INFN Sezione di Trieste ^a, Università di Trieste ^b, Trieste, Italy

S. Belforte^a, V. Candelise^{a,b}, M. Casarsa^a, F. Cossutti^a, A. Da Rold^{a,b}, G. Della Ricca^{a,b}, F. Vazzoler^{a,b}

Kyungpook National University, Daegu, Korea

S. Dogra, C. Huh, B. Kim, D.H. Kim, G.N. Kim, J. Lee, S.W. Lee, C.S. Moon, Y.D. Oh, S.I. Pak, S. Sekmen, Y.C. Yang

Chonnam National University, Institute for Universe and Elementary Particles, Kwangju, Korea

H. Kim, D.H. Moon

Hanyang University, Seoul, Korea

B. Francois, T.J. Kim, J. Park

Korea University, Seoul, Korea

S. Cho, S. Choi, Y. Go, S. Ha, B. Hong, K. Lee, K.S. Lee, J. Lim, J. Park, S.K. Park, J. Yoo

Kyung Hee University, Department of Physics, Seoul, Republic of Korea

J. Goh, A. Gurtu

Sejong University, Seoul, Korea

H.S. Kim, Y. Kim

Seoul National University, Seoul, Korea

J. Almond, J.H. Bhyun, J. Choi, S. Jeon, J. Kim, J.S. Kim, S. Ko, H. Kwon, H. Lee, K. Lee, S. Lee, K. Nam, B.H. Oh, M. Oh, S.B. Oh, B.C. Radburn-Smith, H. Seo, U.K. Yang, I. Yoon

University of Seoul, Seoul, Korea

D. Jeon, J.H. Kim, B. Ko, J.S.H. Lee, I.C. Park, Y. Roh, D. Song, I.J. Watson

Yonsei University, Department of Physics, Seoul, Korea

H.D. Yoo

Sungkyunkwan University, Suwon, Korea

Y. Choi, C. Hwang, Y. Jeong, H. Lee, J. Lee, Y. Lee, I. Yu

Riga Technical University, Riga, Latvia

V. Veckalns⁴¹

Vilnius University, Vilnius, Lithuania

A. Juodagalvis, A. Rinkevicius, G. Tamulaitis

National Centre for Particle Physics, Universiti Malaya, Kuala Lumpur, Malaysia

W.A.T. Wan Abdullah, M.N. Yusli, Z. Zolkapli

Universidad de Sonora (UNISON), Hermosillo, Mexico

J.F. Benitez, A. Castaneda Hernandez, J.A. Murillo Quijada, L. Valencia Palomo

Centro de Investigacion y de Estudios Avanzados del IPN, Mexico City, Mexico

H. Castilla-Valdez, E. De La Cruz-Burelo, I. Heredia-De La Cruz⁴², R. Lopez-Fernandez, A. Sanchez-Hernandez

Universidad Iberoamericana, Mexico City, Mexico

S. Carrillo Moreno, C. Oropeza Barrera, M. Ramirez-Garcia, F. Vazquez Valencia

Benemerita Universidad Autonoma de Puebla, Puebla, Mexico

J. Eysermans, I. Pedraza, H.A. Salazar Ibarguen, C. Uribe Estrada

Universidad Autónoma de San Luis Potosí, San Luis Potosí, Mexico

A. Morelos Pineda

University of Montenegro, Podgorica, Montenegro

J. Mijuskovic⁴, N. Raicevic

University of Auckland, Auckland, New Zealand

D. Krofcheck

University of Canterbury, Christchurch, New Zealand

S. Bheesette, P.H. Butler

National Centre for Physics, Quaid-I-Azam University, Islamabad, Pakistan

A. Ahmad, M.I. Asghar, M.I.M. Awan, Q. Hassan, H.R. Hoorani, W.A. Khan, M.A. Shah, M. Shoaib, M. Waqas

AGH University of Science and Technology Faculty of Computer Science, Electronics and Telecommunications, Krakow, Poland

V. Avati, L. Grzanka, M. Malawski

National Centre for Nuclear Research, Swierk, Poland

H. Bialkowska, M. Bluj, B. Boimska, T. Frueboes, M. Górski, M. Kazana, M. Szeleper, P. Traczyk, P. Zalewski

Institute of Experimental Physics, Faculty of Physics, University of Warsaw, Warsaw, Poland

K. Bunkowski, A. Byszuk⁴³, K. Doroba, A. Kalinowski, M. Konecki, J. Krolikowski, M. Olszewski, M. Walczak

Laboratório de Instrumentação e Física Experimental de Partículas, Lisboa, Portugal

M. Araujo, P. Bargassa, D. Bastos, A. Di Francesco, P. Faccioli, B. Galinhas, M. Gallinaro, J. Hollar, N. Leonardo, T. Niknejad, J. Seixas, K. Shchelina, O. Toldaiev, J. Varela

Joint Institute for Nuclear Research, Dubna, Russia

S. Afanasiev, P. Bunin, M. Gavrilenko, I. Golutvin, I. Gorbunov, A. Kamenev, V. Karjavine, A. Lanev, A. Malakhov, V. Matveev^{44,45}, P. Moisenz, V. Palichik, V. Perelygin, M. Savina, D. Seitova, V. Shalaev, S. Shmatov, S. Shulha, V. Smirnov, O. Teryaev, N. Voytishin, A. Zarubin, I. Zhizhin

Petersburg Nuclear Physics Institute, Gatchina (St. Petersburg), Russia

G. Gavrillov, V. Golovtsov, Y. Ivanov, V. Kim⁴⁶, E. Kuznetsova⁴⁷, V. Murzin, V. Oreshkin, I. Smirnov, D. Sosnov, V. Sulimov, L. Uvarov, S. Volkov, A. Vorobyev

Institute for Nuclear Research, Moscow, Russia

Yu. Andreev, A. Dermenev, S. Gninenko, N. Golubev, A. Karneyeu, M. Kirsanov, N. Krasnikov, A. Pashenkov, G. Pivovarov, D. Tlisov, A. Toropin

Institute for Theoretical and Experimental Physics named by A.I. Alikhanov of NRC 'Kurchatov Institute', Moscow, Russia

V. Epshteyn, V. Gavrillov, N. Lychkovskaya, A. Nikitenko⁴⁸, V. Popov, I. Pozdnyakov, G. Safronov, A. Spiridonov, A. Stepenov, M. Toms, E. Vlasov, A. Zhokin

Moscow Institute of Physics and Technology, Moscow, Russia

T. Aushev

National Research Nuclear University 'Moscow Engineering Physics Institute' (MEPhI), Moscow, Russia

O. Bychkova, R. Chistov⁴⁹, M. Danilov⁴⁹, D. Philippov, S. Polikarpov⁴⁹

P.N. Lebedev Physical Institute, Moscow, Russia

V. Andreev, M. Azarkin, I. Dremin, M. Kirakosyan, A. Terkulov

Skobeltsyn Institute of Nuclear Physics, Lomonosov Moscow State University, Moscow, Russia

A. Belyaev, E. Boos, M. Dubinin⁵⁰, L. Dudko, A. Ershov, A. Gribushin, V. Klyukhin, O. Kodolova, I. Lokhtin, S. Obraztsov, S. Petrushanko, V. Savrin, A. Snigirev

Novosibirsk State University (NSU), Novosibirsk, Russia

V. Blinov⁵¹, T. Dimova⁵¹, L. Kardapoltsev⁵¹, I. Ovtin⁵¹, Y. Skovpen⁵¹

Institute for High Energy Physics of National Research Centre 'Kurchatov Institute', Protvino, Russia

I. Azhgirey, I. Bayshev, V. Kachanov, A. Kalinin, D. Konstantinov, V. Petrov, R. Ryutin, A. Sobol, S. Troshin, N. Tyurin, A. Uzunian, A. Volkov

National Research Tomsk Polytechnic University, Tomsk, Russia

A. Babaev, A. Iuzhakov, V. Okhotnikov, L. Sukhikh

Tomsk State University, Tomsk, Russia

V. Borchsh, V. Ivanchenko, E. Tcherniaev

University of Belgrade: Faculty of Physics and VINCA Institute of Nuclear Sciences, Belgrade, Serbia

P. Adzic⁵², P. Cirkovic, M. Dordevic, P. Milenovic, J. Milosevic

Centro de Investigaciones Energéticas Medioambientales y Tecnológicas (CIEMAT), Madrid, Spain

M. Aguilar-Benitez, J. Alcaraz Maestre, A. Álvarez Fernández, I. Bachiller, M. Barrio Luna, Cristina F. Bedoya, J.A. Brochero Cifuentes, C.A. Carrillo Montoya, M. Cepeda, M. Cerrada, N. Colino, B. De La Cruz, A. Delgado Peris, J.P. Fernández Ramos, J. Flix, M.C. Fouz, O. Gonzalez Lopez, S. Goy Lopez, J.M. Hernandez, M.I. Josa, D. Moran, Á. Navarro Tobar, A. Pérez-Calero Yzquierdo, J. Puerta Pelayo, I. Redondo, L. Romero, S. Sánchez Navas, M.S. Soares, A. Triossi, C. Willmott

Universidad Autónoma de Madrid, Madrid, Spain

C. Albajar, J.F. de Trocóniz, R. Reyes-Almanza

Universidad de Oviedo, Instituto Universitario de Ciencias y Tecnologías Espaciales de Asturias (ICTEA), Oviedo, Spain

B. Alvarez Gonzalez, J. Cuevas, C. Erice, J. Fernandez Menendez, S. Folgueras, I. Gonzalez Caballero, E. Palencia Cortezon, C. Ramón Álvarez, V. Rodríguez Bouza, S. Sanchez Cruz

Instituto de Física de Cantabria (IFCA), CSIC-Universidad de Cantabria, Santander, Spain

I.J. Cabrillo, A. Calderon, B. Chazin Quero, J. Duarte Campderros, M. Fernandez, P.J. Fernández Manteca, A. García Alonso, G. Gomez, C. Martinez Rivero, P. Martinez Ruiz del Arbol, F. Matorras, J. Piedra Gomez, C. Prieels, F. Ricci-Tam, T. Rodrigo, A. Ruiz-Jimeno, L. Russo⁵³, L. Scodellaro, I. Vila, J.M. Vizán Garcia

University of Colombo, Colombo, Sri Lanka

MK Jayananda, B. Kailasapathy⁵⁴, D.U.J. Sonnadara, DDC Wickramarathna

University of Ruhuna, Department of Physics, Matara, Sri Lanka

W.G.D. Dharmaratna, K. Liyanage, N. Perera, N. Wickramage

CERN, European Organization for Nuclear Research, Geneva, Switzerland

T.K. Aarrestad, D. Abbaneo, B. Akgun, E. Auffray, G. Auzinger, J. Baechler, P. Baillon, A.H. Ball, D. Barney, J. Bendavid, N. Beni, M. Bianco, A. Bocci, P. Bortignon, E. Bossini, E. Brondolin, T. Camporesi, G. Cerminara, L. Cristella, D. d'Enterria, A. Dabrowski, N. Daci, V. Daponte, A. David, A. De Roeck, M. Deile, R. Di Maria, M. Dobson, M. Dünser, N. Dupont, A. Elliott-Peisert, N. Emriskova, F. Fallavollita⁵⁵, D. Fasanella, S. Fiorendi, G. Franzoni, J. Fulcher, W. Funk, S. Giani, D. Gigi, K. Gill, F. Glege, L. Gouskos, M. Guilbaud, D. Gulhan, M. Haranko, J. Hegeman, Y. Iiyama, V. Innocente, T. James, P. Janot, J. Kaspar, J. Kieseler, M. Komm, N. Kratochwil, C. Lange, P. Lecoq, K. Long, C. Lourenço, L. Malgeri, M. Mannelli, A. Massironi, F. Meijers, S. Mersi, E. Meschi, F. Moortgat, M. Mulders, J. Ngadiuba, J. Niedziela, S. Orfanelli, L. Orsini, F. Pantaleo¹⁹, L. Pape, E. Perez, M. Peruzzi, A. Petrilli, G. Petrucciani, A. Pfeiffer, M. Pierini, D. Rabad, A. Racz, M. Rieger, M. Rovere, H. Sakulin, J. Salfeld-Nebgen, S. Scarfi, C. Schäfer, C. Schwick, M. Selvaggi, A. Sharma, P. Silva, W. Snoeys, P. Sphicas⁵⁶, J. Steggemann, S. Summers, V.R. Tavolaro, D. Treille, A. Tsiro, G.P. Van Onsem, A. Vartak, M. Verzetti, K.A. Wozniak, W.D. Zeuner

Paul Scherrer Institut, Villigen, Switzerland

L. Caminada⁵⁷, W. Erdmann, R. Horisberger, Q. Ingram, H.C. Kaestli, D. Kotlinski, U. Langenegger, T. Rohe

ETH Zurich - Institute for Particle Physics and Astrophysics (IPA), Zurich, Switzerland

M. Backhaus, P. Berger, A. Calandri, N. Chernyavskaya, G. Dissertori, M. Dittmar, M. Donegà, C. Dorfer, T. Gadek, T.A. Gómez Espinosa, C. Grab, D. Hits, W. Lustermann, A.-M. Lyon, R.A. Manzoni, M.T. Meinhard, F. Micheli, P. Musella, F. Nessi-Tedaldi, F. Pauss, V. Perovic,

G. Perrin, L. Perrozzi, S. Pigazzini, M.G. Ratti, M. Reichmann, C. Reissel, T. Reitenspiess, B. Ristic, D. Ruini, D.A. Sanz Becerra, M. Schönenberger, L. Shchutska, V. Stampf, M.L. Vesterbacka Olsson, R. Wallny, D.H. Zhu

Universität Zürich, Zurich, Switzerland

C. Amsler⁵⁸, C. Botta, D. Brzhechko, M.F. Canelli, A. De Cosa, R. Del Burgo, J.K. Heikkilä, M. Huwiler, A. Jofrehei, B. Kilminster, S. Leontsinis, A. Macchiolo, P. Meiring, V.M. Mikuni, U. Molinatti, I. Neutelings, G. Rauco, A. Reimers, P. Robmann, K. Schweiger, Y. Takahashi, S. Wertz

National Central University, Chung-Li, Taiwan

C. Adloff⁵⁹, C.M. Kuo, W. Lin, A. Roy, T. Sarkar³⁴, S.S. Yu

National Taiwan University (NTU), Taipei, Taiwan

L. Ceard, P. Chang, Y. Chao, K.F. Chen, P.H. Chen, W.-S. Hou, Y.y. Li, R.-S. Lu, E. Paganis, A. Psallidas, A. Steen, E. Yazgan

Chulalongkorn University, Faculty of Science, Department of Physics, Bangkok, Thailand

B. Asavapibhop, C. Asawatangtrakuldee, N. Srimanobhas

Çukurova University, Physics Department, Science and Art Faculty, Adana, Turkey

F. Boran, S. Damarseckin⁶⁰, Z.S. Demiroglu, F. Dolek, C. Dozen⁶¹, I. Dumanoglu⁶², E. Eskut, G. Gokbulut, Y. Guler, E. Gurpinar Guler⁶³, I. Hos⁶⁴, C. Isik, E.E. Kangal⁶⁵, O. Kara, A. Kayis Topaksu, U. Kiminsu, G. Onengut, K. Ozdemir⁶⁶, A. Polatoz, A.E. Simsek, B. Tali⁶⁷, U.G. Tok, S. Turkcapar, I.S. Zorbakir, C. Zorbilmez

Middle East Technical University, Physics Department, Ankara, Turkey

B. Isildak⁶⁸, G. Karapinar⁶⁹, K. Ocalan⁷⁰, M. Yalvac⁷¹

Bogazici University, Istanbul, Turkey

I.O. Atakisi, E. Gülmez, M. Kaya⁷², O. Kaya⁷³, Ö. Özçelik, S. Tekten⁷⁴, E.A. Yetkin⁷⁵

Istanbul Technical University, Istanbul, Turkey

A. Cakir, K. Cankocak⁶², Y. Komurcu, S. Sen⁷⁶

Istanbul University, Istanbul, Turkey

F. Aydogmus Sen, S. Cerci⁶⁷, B. Kaynak, S. Ozkorucuklu, D. Sunar Cerci⁶⁷

Institute for Scintillation Materials of National Academy of Science of Ukraine, Kharkov, Ukraine

B. Grynyov

National Scientific Center, Kharkov Institute of Physics and Technology, Kharkov, Ukraine

L. Levchuk

University of Bristol, Bristol, United Kingdom

E. Bhal, S. Bologna, J.J. Brooke, D. Burns⁷⁷, E. Clement, D. Cussans, H. Flacher, J. Goldstein, G.P. Heath, H.F. Heath, L. Kreczko, B. Krikler, S. Paramesvaran, T. Sakuma, S. Seif El Nasr-Storey, V.J. Smith, J. Taylor, A. Titterton

Rutherford Appleton Laboratory, Didcot, United Kingdom

K.W. Bell, A. Belyaev⁷⁸, C. Brew, R.M. Brown, D.J.A. Cockerill, K.V. Ellis, K. Harder, S. Harper, J. Linacre, K. Manolopoulos, D.M. Newbold, E. Olaiya, D. Petyt, T. Reis, T. Schuh, C.H. Shepherd-Themistocleous, A. Thea, I.R. Tomalin, T. Williams

Imperial College, London, United Kingdom

R. Bainbridge, P. Bloch, S. Bonomally, J. Borg, S. Breeze, O. Buchmuller, A. Bundock, V. Cepaitis, G.S. Chahal⁷⁹, D. Colling, P. Dauncey, G. Davies, M. Della Negra, P. Everaerts, G. Fedi, G. Hall, G. Iles, J. Langford, L. Lyons, A.-M. Magnan, S. Malik, A. Martelli, V. Milosevic, J. Nash⁸⁰, V. Palladino, M. Pesaresi, D.M. Raymond, A. Richards, A. Rose, E. Scott, C. Seez, A. Shtipliyski, M. Stoye, A. Tapper, K. Uchida, T. Virdee¹⁹, N. Wardle, S.N. Webb, D. Winterbottom, A.G. Zecchinelli, S.C. Zenz

Brunel University, Uxbridge, United Kingdom

J.E. Cole, P.R. Hobson, A. Khan, P. Kyberd, C.K. Mackay, I.D. Reid, L. Teodorescu, S. Zahid

Baylor University, Waco, USA

A. Brinkerhoff, K. Call, B. Caraway, J. Dittmann, K. Hatakeyama, A.R. Kanuganti, C. Madrid, B. McMaster, N. Pastika, S. Sawant, C. Smith

Catholic University of America, Washington, DC, USA

R. Bartek, A. Dominguez, R. Uniyal, A.M. Vargas Hernandez

The University of Alabama, Tuscaloosa, USA

A. Buccilli, O. Charaf, S.I. Cooper, S.V. Gleyzer, C. Henderson, P. Rumerio, C. West

Boston University, Boston, USA

A. Akpinar, A. Albert, D. Arcaro, C. Cosby, Z. Demiragli, D. Gastler, C. Richardson, J. Rohlf, K. Salyer, D. Sperka, D. Spitzbart, I. Suarez, S. Yuan, D. Zou

Brown University, Providence, USA

G. Benelli, B. Burkle, X. Coubez²⁰, D. Cutts, Y.t. Duh, M. Hadley, U. Heintz, J.M. Hogan⁸¹, K.H.M. Kwok, E. Laird, G. Landsberg, K.T. Lau, J. Lee, M. Narain, S. Sagir⁸², R. Syarif, E. Usai, W.Y. Wong, D. Yu, W. Zhang

University of California, Davis, Davis, USA

R. Band, C. Brainerd, R. Breedon, M. Calderon De La Barca Sanchez, M. Chertok, J. Conway, R. Conway, P.T. Cox, R. Erbacher, C. Flores, G. Funk, F. Jensen, W. Ko[†], O. Kukral, R. Lander, M. Mulhearn, D. Pellett, J. Pilot, M. Shi, D. Taylor, K. Tos, M. Tripathi, Y. Yao, F. Zhang

University of California, Los Angeles, USA

M. Bachtis, C. Bravo, R. Cousins, A. Dasgupta, A. Florent, D. Hamilton, J. Hauser, M. Ignatenko, T. Lam, N. Mccoll, W.A. Nash, S. Regnard, D. Saltzberg, C. Schnaible, B. Stone, V. Valuev

University of California, Riverside, Riverside, USA

K. Burt, Y. Chen, R. Clare, J.W. Gary, S.M.A. Ghiasi Shirazi, G. Hanson, G. Karapostoli, O.R. Long, N. Manganelli, M. Olmedo Negrete, M.I. Paneva, W. Si, S. Wimpenny, Y. Zhang

University of California, San Diego, La Jolla, USA

J.G. Branson, P. Chang, S. Cittolin, S. Cooperstein, N. Deelen, M. Derdzinski, J. Duarte, R. Gerosa, D. Gilbert, B. Hashemi, D. Klein, V. Krutelyov, J. Letts, M. Masciovecchio, S. May, S. Padhi, M. Pieri, V. Sharma, M. Tadel, F. Würthwein, A. Yagil

University of California, Santa Barbara - Department of Physics, Santa Barbara, USA

N. Amin, R. Bhandari, C. Campagnari, M. Citron, A. Dorsett, V. Dutta, J. Incandela, B. Marsh, H. Mei, A. Ovcharova, H. Qu, M. Quinnan, J. Richman, U. Sarica, D. Stuart, S. Wang

California Institute of Technology, Pasadena, USA

D. Anderson, A. Bornheim, O. Cerri, I. Dutta, J.M. Lawhorn, N. Lu, J. Mao, H.B. Newman, T.Q. Nguyen, J. Pata, M. Spiropulu, J.R. Vlimant, S. Xie, Z. Zhang, R.Y. Zhu

Carnegie Mellon University, Pittsburgh, USA

J. Alison, M.B. Andrews, T. Ferguson, T. Mudholkar, M. Paulini, M. Sun, I. Vorobiev, M. Weinberg

University of Colorado Boulder, Boulder, USA

J.P. Cumalat, W.T. Ford, E. MacDonald, T. Mulholland, R. Patel, A. Perloff, K. Stenson, K.A. Ulmer, S.R. Wagner

Cornell University, Ithaca, USA

J. Alexander, Y. Cheng, J. Chu, D.J. Cranshaw, A. Datta, A. Frankenthal, K. Mcdermott, J. Monroy, J.R. Patterson, D. Quach, A. Ryd, W. Sun, S.M. Tan, Z. Tao, J. Thom, P. Wittich, M. Zientek

Fermi National Accelerator Laboratory, Batavia, USA

S. Abdullin, M. Albrow, M. Alyari, G. Apollinari, A. Apresyan, A. Apyan, S. Banerjee, L.A.T. Bauerdick, A. Beretvas, D. Berry, J. Berryhill, P.C. Bhat, K. Burkett, J.N. Butler, A. Canepa, G.B. Cerati, H.W.K. Cheung, F. Chlebana, M. Cremonesi, V.D. Elvira, J. Freeman, Z. Gecse, E. Gottschalk, L. Gray, D. Green, S. Grünendahl, O. Gutsche, R.M. Harris, S. Hasegawa, R. Heller, T.C. Herwig, J. Hirschauer, B. Jayatilaka, S. Jindariani, M. Johnson, U. Joshi, T. Klijnsma, B. Klima, M.J. Kortelainen, S. Lammel, J. Lewis, D. Lincoln, R. Lipton, M. Liu, T. Liu, J. Lykken, K. Maeshima, D. Mason, P. McBride, P. Merkel, S. Mrenna, S. Nahn, V. O'Dell, V. Papadimitriou, K. Pedro, C. Pena⁵⁰, O. Prokofyev, F. Ravera, A. Reinsvold Hall, L. Ristori, B. Schneider, E. Sexton-Kennedy, N. Smith, A. Soha, W.J. Spalding, L. Spiegel, S. Stoynev, J. Strait, L. Taylor, S. Tkaczyk, N.V. Tran, L. Uplegger, E.W. Vaandering, M. Wang, H.A. Weber, A. Woodard

University of Florida, Gainesville, USA

D. Acosta, P. Avery, D. Bourilkov, L. Cadamuro, V. Cherepanov, F. Errico, R.D. Field, D. Guerrero, B.M. Joshi, M. Kim, J. Konigsberg, A. Korytov, K.H. Lo, K. Matchev, N. Menendez, G. Mitselmakher, D. Rosenzweig, K. Shi, J. Wang, S. Wang, X. Zuo

Florida International University, Miami, USA

Y.R. Joshi

Florida State University, Tallahassee, USA

T. Adams, A. Askew, D. Diaz, R. Habibullah, S. Hagopian, V. Hagopian, K.F. Johnson, R. Khurana, T. Kolberg, G. Martinez, H. Prosper, C. Schiber, R. Yohay, J. Zhang

Florida Institute of Technology, Melbourne, USA

M.M. Baarmand, S. Butalla, T. Elkafrawy¹⁴, M. Hohlmann, D. Noonan, M. Rahmani, M. Saunders, F. Yumiceva

University of Illinois at Chicago (UIC), Chicago, USA

M.R. Adams, L. Apanasevich, H. Becerril Gonzalez, R. Cavanaugh, X. Chen, S. Dittmer, O. Evdokimov, C.E. Gerber, D.A. Hangal, D.J. Hofman, C. Mills, G. Oh, T. Roy, M.B. Tonjes, N. Varelas, J. Viinikainen, H. Wang, X. Wang, Z. Wu

The University of Iowa, Iowa City, USA

M. Alhousseini, B. Bilki⁶³, K. Dilsiz⁸³, S. Durgut, R.P. Gandrajula, M. Haytmyradov, V. Khristenko, O.K. Köseyan, J.-P. Merlo, A. Mestvirishvili⁸⁴, A. Moeller, J. Nachtman, H. Ogul⁸⁵, Y. Onel, F. Ozok⁸⁶, A. Penzo, C. Snyder, E. Tiras, J. Wetzel, K. Yi⁸⁷

Johns Hopkins University, Baltimore, USA

O. Amram, B. Blumenfeld, L. Corcodilos, M. Eminizer, A.V. Gritsan, S. Kyriacou, P. Maksimovic, C. Mantilla, J. Roskes, M. Swartz, T.Á. Vámi

The University of Kansas, Lawrence, USA

C. Baldenegro Barrera, P. Baringer, A. Bean, A. Bylinkin, T. Isidori, S. Khalil, J. King, G. Krintiras, A. Kropivnitskaya, C. Lindsey, N. Minafra, M. Murray, C. Rogan, C. Royon, S. Sanders, E. Schmitz, J.D. Tapia Takaki, Q. Wang, J. Williams, G. Wilson

Kansas State University, Manhattan, USA

S. Duric, A. Ivanov, K. Kaadze, D. Kim, Y. Maravin, D.R. Mendis, T. Mitchell, A. Modak, A. Mohammadi

Lawrence Livermore National Laboratory, Livermore, USA

F. Rebassoo, D. Wright

University of Maryland, College Park, USA

E. Adams, A. Baden, O. Baron, A. Belloni, S.C. Eno, Y. Feng, N.J. Hadley, S. Jabeen, G.Y. Jeng, R.G. Kellogg, T. Koeth, A.C. Mignerey, S. Nabili, M. Seidel, A. Skuja, S.C. Tonwar, L. Wang, K. Wong

Massachusetts Institute of Technology, Cambridge, USA

D. Abercrombie, B. Allen, R. Bi, S. Brandt, W. Busza, I.A. Cali, Y. Chen, M. D'Alfonso, G. Gomez Ceballos, M. Goncharov, P. Harris, D. Hsu, M. Hu, M. Klute, D. Kovalskyi, J. Krupa, Y.-J. Lee, P.D. Luckey, B. Maier, A.C. Marini, C. McGinn, C. Mironov, S. Narayanan, X. Niu, C. Paus, D. Rankin, C. Roland, G. Roland, Z. Shi, G.S.F. Stephans, K. Sumorok, K. Tatar, D. Velicanu, J. Wang, T.W. Wang, Z. Wang, B. Wyslouch

University of Minnesota, Minneapolis, USA

R.M. Chatterjee, A. Evans, S. Guts[†], P. Hansen, J. Hiltbrand, Sh. Jain, M. Krohn, Y. Kubota, Z. Lesko, J. Mans, M. Revering, R. Rusack, R. Saradhy, N. Schroeder, N. Strobbe, M.A. Wadud

University of Mississippi, Oxford, USA

J.G. Acosta, S. Oliveros

University of Nebraska-Lincoln, Lincoln, USA

K. Bloom, S. Chauhan, D.R. Claes, C. Fangmeier, L. Finco, F. Golf, J.R. González Fernández, I. Kravchenko, J.E. Siado, G.R. Snow[†], B. Stieger, W. Tabb

State University of New York at Buffalo, Buffalo, USA

G. Agarwal, C. Harrington, L. Hay, I. Iashvili, A. Kharchilava, C. McLean, D. Nguyen, A. Parker, J. Pekkanen, S. Rappoccio, B. Roozbahani

Northeastern University, Boston, USA

G. Alverson, E. Barberis, C. Freer, Y. Haddad, A. Hortiangtham, G. Madigan, B. Marzocchi, D.M. Morse, V. Nguyen, T. Orimoto, L. Skinnari, A. Tishelman-Charny, T. Wamorkar, B. Wang, A. Wisecarver, D. Wood

Northwestern University, Evanston, USA

S. Bhattacharya, J. Bueghly, Z. Chen, A. Gilbert, T. Gunter, K.A. Hahn, N. Odell, M.H. Schmitt, K. Sung, M. Velasco

University of Notre Dame, Notre Dame, USA

R. Bucci, N. Dev, R. Goldouzian, M. Hildreth, K. Hurtado Anampa, C. Jessop, D.J. Karmgard, K. Lannon, W. Li, N. Loukas, N. Marinelli, I. Mcalister, F. Meng, K. Mohrman, Y. Musienko⁴⁴, R. Ruchti, P. Siddireddy, S. Taroni, M. Wayne, A. Wightman, M. Wolf, L. Zygala

The Ohio State University, Columbus, USA

J. Alimena, B. Bylsma, B. Cardwell, L.S. Durkin, B. Francis, C. Hill, W. Ji, A. Lefeld, B.L. Winer, B.R. Yates

Princeton University, Princeton, USA

G. Dezoort, P. Elmer, B. Greenberg, N. Haubrich, S. Higginbotham, A. Kalogeropoulos, G. Kopp, S. Kwan, D. Lange, M.T. Lucchini, J. Luo, D. Marlow, K. Mei, I. Ojalvo, J. Olsen, C. Palmer, P. Piroué, D. Stickland, C. Tully

University of Puerto Rico, Mayaguez, USA

S. Malik, S. Norberg

Purdue University, West Lafayette, USA

V.E. Barnes, R. Chawla, S. Das, L. Gutay, M. Jones, A.W. Jung, B. Mahakud, G. Negro, N. Neumeister, C.C. Peng, S. Piperov, H. Qiu, J.F. Schulte, N. Trevisani, F. Wang, R. Xiao, W. Xie

Purdue University Northwest, Hammond, USA

T. Cheng, J. Dolen, N. Parashar, M. Stojanovic

Rice University, Houston, USA

A. Baty, S. Dildick, K.M. Ecklund, S. Freed, F.J.M. Geurts, M. Kilpatrick, A. Kumar, W. Li, B.P. Padley, R. Redjimi, J. Roberts[†], J. Rorie, W. Shi, A.G. Stahl Leiton, Z. Tu, A. Zhang

University of Rochester, Rochester, USA

A. Bodek, P. de Barbaro, R. Demina, J.L. Dulemba, C. Fallon, T. Ferbel, M. Galanti, A. Garcia-Bellido, O. Hindrichs, A. Khukhunaishvili, E. Ranken, R. Taus

Rutgers, The State University of New Jersey, Piscataway, USA

B. Chiarito, J.P. Chou, A. Gandrakota, Y. Gershtein, E. Halkiadakis, A. Hart, M. Heindl, E. Hughes, S. Kaplan, O. Karacheban²³, I. Laflotte, A. Lath, R. Montalvo, K. Nash, M. Osherson, S. Salur, S. Schnetzer, S. Somalwar, R. Stone, S.A. Thayil, S. Thomas

University of Tennessee, Knoxville, USA

H. Acharya, A.G. Delannoy, S. Spanier

Texas A&M University, College Station, USA

O. Bouhali⁸⁸, M. Dalchenko, A. Delgado, R. Eusebi, J. Gilmore, T. Huang, T. Kamon⁸⁹, H. Kim, S. Luo, S. Malhotra, R. Mueller, D. Overton, L. Perniè, D. Rathjens, A. Safonov

Texas Tech University, Lubbock, USA

N. Akchurin, J. Damgov, V. Hegde, S. Kunori, K. Lamichhane, S.W. Lee, T. Mengke, S. Muthumuni, T. Peltola, S. Undleeb, I. Volobouev, Z. Wang, A. Whitbeck

Vanderbilt University, Nashville, USA

E. Appelt, S. Greene, A. Gurrola, R. Janjam, W. Johns, C. Maguire, A. Melo, H. Ni, K. Padeken, F. Romeo, P. Sheldon, S. Tuo, J. Velkovska, M. Verweij

University of Virginia, Charlottesville, USA

L. Ang, M.W. Arenton, B. Cox, G. Cummings, J. Hakala, R. Hirosky, M. Joyce, A. Ledovskoy, C. Neu, B. Tannenwald, Y. Wang, E. Wolfe, F. Xia

Wayne State University, Detroit, USA

P.E. Karchin, N. Poudyal, J. Sturdy, P. Thapa

University of Wisconsin - Madison, Madison, WI, USA

K. Black, T. Bose, J. Buchanan, C. Caillol, S. Dasu, I. De Bruyn, L. Dodd, C. Galloni,

H. He, M. Herndon, A. Hervé, U. Hussain, A. Lanaro, A. Loeliger, R. Loveless, J. Madhusudanan Sreekala, A. Mallampalli, D. Pinna, T. Ruggles, A. Savin, V. Shang, V. Sharma, W.H. Smith, D. Teague, S. Trembath-reichert, W. Vetens

†: Deceased

- 1: Also at Vienna University of Technology, Vienna, Austria
- 2: Also at Department of Basic and Applied Sciences, Faculty of Engineering, Arab Academy for Science, Technology and Maritime Transport, Alexandria, Egypt
- 3: Also at Université Libre de Bruxelles, Bruxelles, Belgium
- 4: Also at IRFU, CEA, Université Paris-Saclay, Gif-sur-Yvette, France
- 5: Also at Universidade Estadual de Campinas, Campinas, Brazil
- 6: Also at Federal University of Rio Grande do Sul, Porto Alegre, Brazil
- 7: Also at UFMS, Nova Andradina, Brazil
- 8: Also at Universidade Federal de Pelotas, Pelotas, Brazil
- 9: Also at University of Chinese Academy of Sciences, Beijing, China
- 10: Also at Institute for Theoretical and Experimental Physics named by A.I. Alikhanov of NRC 'Kurchatov Institute', Moscow, Russia
- 11: Also at Joint Institute for Nuclear Research, Dubna, Russia
- 12: Also at Helwan University, Cairo, Egypt
- 13: Now at Zewail City of Science and Technology, Zewail, Egypt
- 14: Also at Ain Shams University, Cairo, Egypt
- 15: Also at Purdue University, West Lafayette, USA
- 16: Also at Université de Haute Alsace, Mulhouse, France
- 17: Also at Tbilisi State University, Tbilisi, Georgia
- 18: Also at Erzincan Binali Yildirim University, Erzincan, Turkey
- 19: Also at CERN, European Organization for Nuclear Research, Geneva, Switzerland
- 20: Also at RWTH Aachen University, III. Physikalisches Institut A, Aachen, Germany
- 21: Also at University of Hamburg, Hamburg, Germany
- 22: Also at Department of Physics, Isfahan University of Technology, Isfahan, Iran, Isfahan, Iran
- 23: Also at Brandenburg University of Technology, Cottbus, Germany
- 24: Also at Skobeltsyn Institute of Nuclear Physics, Lomonosov Moscow State University, Moscow, Russia
- 25: Also at Institute of Physics, University of Debrecen, Debrecen, Hungary, Debrecen, Hungary
- 26: Also at Physics Department, Faculty of Science, Assiut University, Assiut, Egypt
- 27: Also at MTA-ELTE Lendület CMS Particle and Nuclear Physics Group, Eötvös Loránd University, Budapest, Hungary, Budapest, Hungary
- 28: Also at Institute of Nuclear Research ATOMKI, Debrecen, Hungary
- 29: Also at IIT Bhubaneswar, Bhubaneswar, India, Bhubaneswar, India
- 30: Also at Institute of Physics, Bhubaneswar, India
- 31: Also at G.H.G. Khalsa College, Punjab, India
- 32: Also at Shoolini University, Solan, India
- 33: Also at University of Hyderabad, Hyderabad, India
- 34: Also at University of Visva-Bharati, Santiniketan, India
- 35: Also at Indian Institute of Technology (IIT), Mumbai, India
- 36: Also at Deutsches Elektronen-Synchrotron, Hamburg, Germany
- 37: Also at Department of Physics, University of Science and Technology of Mazandaran, Behshahr, Iran
- 38: Now at INFN Sezione di Bari ^a, Università di Bari ^b, Politecnico di Bari ^c, Bari, Italy

-
- 39: Also at Italian National Agency for New Technologies, Energy and Sustainable Economic Development, Bologna, Italy
- 40: Also at Centro Siciliano di Fisica Nucleare e di Struttura Della Materia, Catania, Italy
- 41: Also at Riga Technical University, Riga, Latvia, Riga, Latvia
- 42: Also at Consejo Nacional de Ciencia y Tecnología, Mexico City, Mexico
- 43: Also at Warsaw University of Technology, Institute of Electronic Systems, Warsaw, Poland
- 44: Also at Institute for Nuclear Research, Moscow, Russia
- 45: Now at National Research Nuclear University 'Moscow Engineering Physics Institute' (MEPhI), Moscow, Russia
- 46: Also at St. Petersburg State Polytechnical University, St. Petersburg, Russia
- 47: Also at University of Florida, Gainesville, USA
- 48: Also at Imperial College, London, United Kingdom
- 49: Also at P.N. Lebedev Physical Institute, Moscow, Russia
- 50: Also at California Institute of Technology, Pasadena, USA
- 51: Also at Budker Institute of Nuclear Physics, Novosibirsk, Russia
- 52: Also at Faculty of Physics, University of Belgrade, Belgrade, Serbia
- 53: Also at Università degli Studi di Siena, Siena, Italy
- 54: Also at Trincomalee Campus, Eastern University, Sri Lanka, Nilaveli, Sri Lanka
- 55: Also at INFN Sezione di Pavia ^a, Università di Pavia ^b, Pavia, Italy, Pavia, Italy
- 56: Also at National and Kapodistrian University of Athens, Athens, Greece
- 57: Also at Universität Zürich, Zurich, Switzerland
- 58: Also at Stefan Meyer Institute for Subatomic Physics, Vienna, Austria, Vienna, Austria
- 59: Also at Laboratoire d'Annecy-le-Vieux de Physique des Particules, IN2P3-CNRS, Annecy-le-Vieux, France
- 60: Also at Şırnak University, Şırnak, Turkey
- 61: Also at Department of Physics, Tsinghua University, Beijing, China, Beijing, China
- 62: Also at Near East University, Research Center of Experimental Health Science, Nicosia, Turkey
- 63: Also at Beykent University, Istanbul, Turkey, Istanbul, Turkey
- 64: Also at Istanbul Aydın University, Application and Research Center for Advanced Studies (App. & Res. Cent. for Advanced Studies), Istanbul, Turkey
- 65: Also at Mersin University, Mersin, Turkey
- 66: Also at Piri Reis University, Istanbul, Turkey
- 67: Also at Adiyaman University, Adiyaman, Turkey
- 68: Also at Ozyegin University, Istanbul, Turkey
- 69: Also at Izmir Institute of Technology, Izmir, Turkey
- 70: Also at Necmettin Erbakan University, Konya, Turkey
- 71: Also at Bozok Universititesi Rektörlüğü, Yozgat, Turkey
- 72: Also at Marmara University, Istanbul, Turkey
- 73: Also at Milli Savunma University, Istanbul, Turkey
- 74: Also at Kafkas University, Kars, Turkey
- 75: Also at Istanbul Bilgi University, Istanbul, Turkey
- 76: Also at Hacettepe University, Ankara, Turkey
- 77: Also at Vrije Universiteit Brussel, Brussel, Belgium
- 78: Also at School of Physics and Astronomy, University of Southampton, Southampton, United Kingdom
- 79: Also at IPPP Durham University, Durham, United Kingdom
- 80: Also at Monash University, Faculty of Science, Clayton, Australia
- 81: Also at Bethel University, St. Paul, Minneapolis, USA, St. Paul, USA

82: Also at Karamanoğlu Mehmetbey University, Karaman, Turkey

83: Also at Bingöl University, Bingöl, Turkey

84: Also at Georgian Technical University, Tbilisi, Georgia

85: Also at Sinop University, Sinop, Turkey

86: Also at Mimar Sinan University, Istanbul, Istanbul, Turkey

87: Also at Nanjing Normal University Department of Physics, Nanjing, China

88: Also at Texas A&M University at Qatar, Doha, Qatar

89: Also at Kyungpook National University, Daegu, Korea, Daegu, Korea